1997

# Phase Structures And Transitions In Thermotropic Liquid Crystals

Peter J. Collings
*Swarthmore College*, pcollin1@swarthmore.edu

CHAPTER 4

# Phase Structures and Transitions in Thermotropic Liquid Crystals

PETER J. COLLINGS

## 4.1 PHASE STRUCTURES

### 4.1.1 Nematic Liquid Crystals

#### 4.1.1.1 Orientational Order

Since there is no long-range positional order in nematic liquid crystals, one is concerned exclusively with long-range orientational order. This is best described by an orientational distribution function, $f(\Omega)$, which is proportional to the probability of finding the long axis of a molecule oriented at solid angle $\Omega$ relative to a coordinate frame in which the $z$-axis points along the director, $\hat{n}$. Since the nematic phase is almost always uniaxial, $f(\Omega)$ does not depend on the azimuthal angle $\phi$, but only on the polar angle $\theta$. Therefore, complete knowledge of the long-range orientational order in a nematic liquid crystal comes from knowledge of the orientational distribution function, $f(\theta)$.

In order to generate an order parameter, averages of certain functions must be used. Since the director in a nematic liquid crystal can point in either of two directions, a logical choice for these functions is the even members of the series of Legendre polynomials:

$$\begin{aligned} P_2(\cos\theta) &= \tfrac{3}{2}\cos^2\theta - \tfrac{1}{2} \\ P_4(\cos\theta) &= \tfrac{1}{8}(35\cos^4\theta - 30\cos^2\theta + 3). \end{aligned} \tag{4.1}$$

The average of $P_2(\cos\theta)$ is called the orientation order parameter and given the symbol $S$.

$$S = \int_0^{\pi} \left(\frac{3}{2}\cos^2\theta - \frac{1}{2}\right)\sin\theta\,\mathrm{d}\theta \Big/ \int_0^{\pi} \sin\theta\,\mathrm{d}\theta. \tag{4.2}$$

If the molecules are perfectly ordered, then $S = 1$. If the molecules are randomly ordered as is true for the isotropic liquid phase, $S = 0$. The orientational order parameter can be determined using just about any method which measures the macroscopic anisotropy of the liquid crystal. This is described in the next

paragraph. The average of $P_4(\cos\theta)$ can be measured by Raman scattering, elastic x-ray and neutron scattering, and by electron spin resonance. These methods give somewhat conflicting results, but seem to indicate that $P_4(\cos\theta)$ starts out small or even negative near the isotropic transition and grows more positive as the temperature is decreased (Jen et al., 1977; Miyano, 1978; Kohli et al., 1976; and Luckhurst and Yeates, 1976).

The relationship between the order parameter and the anisotropy of a macroscopic property can be illustrated quite easily. Let $T_{xx}$, $T_{yy}$, and $T_{zz}$ be the three components of a molecular tensor property, such as the diamagnetic susceptibility. Let $T'_{x'x'}$, $T'_{y'y'}$, and $T'_{z'z'}$ be the components of the corresponding macroscopic tensor property, with the z'-axis along the director. If the direction cosines giving the orientation of molecular axis $i$ relative to macroscopic direction $i'$ are denoted by $A_{i'i}$ then the transformations relating $T_{ij}$ to $T_{i'j'}$ are as follows.

$$\begin{aligned}
\langle T'_{x'x'}\rangle &= \langle A^2_{x'x}\rangle\langle T_{xx}\rangle + \langle A^2_{x'y}\rangle\langle T_{yy}\rangle + \langle A^2_{x'z}\rangle\langle T_{zz}\rangle \\
\langle T'_{y'y'}\rangle &= \langle A^2_{y'x}\rangle\langle T_{xx}\rangle + \langle A^2_{y'y}\rangle\langle T_{yy}\rangle + \langle A^2_{y'z}\rangle\langle T_{zz}\rangle \\
\langle T'_{z'z'}\rangle &= \langle A^2_{z'x}\rangle\langle T_{xx}\rangle + \langle A^2_{z'y}\rangle\langle T_{yy}\rangle + \langle A^2_{z'z}\rangle\langle T_{zz}\rangle.
\end{aligned} \tag{4.3}$$

The brackets denote an average over time and an assumption has been made that the intramolecular and intermolecular motions are uncorrelated. Equation (4.3) allows the relationship between the anisotropies in the microscopic and macroscopic properties to be determined.

$$\begin{aligned}
\langle \Delta T'\rangle &= \langle T_{z'z'}\rangle - \tfrac{1}{2}(\langle T'_{x'x'}\rangle + \langle T'_{y'y'}\rangle) \\
\langle \Delta T'\rangle &= \tfrac{3}{2}(\langle A^2_{z'x}\rangle\langle T_{xx}\rangle + \langle A^2_{z'y}\rangle\langle T_{yy}\rangle \\
&\quad + \langle A^2_{z'z}\rangle\langle T_{zz}\rangle) - \tfrac{1}{2}\mathrm{Tr}\langle \overleftrightarrow{T}\rangle.
\end{aligned} \tag{4.4}$$

If three order parameters are defined as follows,

$$\begin{aligned}
S_{xx} &= \tfrac{3}{2}\langle A^2_{z'x}\rangle - \tfrac{1}{2} \qquad S_{yy} = \tfrac{3}{2}\langle A^2_{z'y}\rangle - \tfrac{1}{2} \\
S_{zz} &= \tfrac{3}{2}\langle A^2_{z'z}\rangle - \tfrac{1}{2}
\end{aligned} \tag{4.5}$$

then the anisotropy can be written in terms of these order parameters. In fact, the sum of these three order parameters is zero, so that only two are necessary to describe the relationship between macroscopic and microscopic tensor properties. The usual choice for the two independent order parameters is $S = S_{zz}$, the orientational order parameter described previously, and $D = S_{yy} - S_{xx}$. With these choices, the macroscopic anisotropy has a simple form:

$$\begin{aligned}
\langle \Delta T'\rangle &= (\langle T_{zz}\rangle - \tfrac{1}{2}[\langle T_{xx}\rangle + \langle T_{yy}\rangle])S \\
&\quad + (\langle T_{yy}\rangle - \langle T_{xx}\rangle)D.
\end{aligned} \tag{4.6}$$

As noted before, $S$ measures the tendency for the longest axis of the molecule to project along $\hat{n}$, while $D$ measures the difference in tendencies for the two transverse molecular axes to project along $\hat{n}$.

Macroscopic properties for which this approach has been used include magnetic susceptibility, electric polarizability, dipolar and quadrupolar NMR, linear dichroism, Raman scattering, birefringence, and EPR. Since the molecular quantities in the parentheses of (4.6) must be known in order to determine the order parameter, some methods are more useful than others (de Gennes and Prost, 1993). Quadrupolar NMR also allows the order parameter for different parts of the molecule to be measured. For example, order parameters for parts of the hydrocarbon chain on the end of liquid crystal molecules tend to decrease the further away they are from the molecular core (Emsley, 1985).

Theoretically, noncylindrically symmetric molecules can form a biaxial nematic phase, that is, one in which all directions perpendicular to the director are not equivalent (Chandrasekhar, 1992). Such a phase has been found in both lyotropic (Yu and Saupe, 1980) and thermotropic systems (Praefcke et al., 1991).

#### 4.1.1.2 Short-Range Positional Order

Positional order is best described through the density–density correlation function ($\rho$ is the density):

$$G(\vec{r} - \vec{r}') = \langle \rho(\vec{r})\rho(\vec{r}')\rangle - \bar{\rho}^2. \tag{4.7}$$

When this correlation function does not decay to zero as $\vec{r} - \vec{r}' \to \infty$, then true long-range order is present. If the correlation function decays to zero as $|\vec{r} - \vec{r}'|^{-\eta}$, where $\eta$ may be temperature-dependent, then the positional order is quasi-long-range. Finally, when the decay of the correlation function is exponential, $e^{-|\vec{r}-\vec{r}'|/\xi}$, where $\xi$ is a correlation length, then the order is short-range only. Long-range order is typical of solids, short-range order is the norm for liquids, and all three forms of positional order are found in liquid crystals (Pershan, 1988).

X-ray scattering is the most valuable tool in measuring the positional order in liquid crystals. High resolution, intense sources, and the ability to produce monodomain samples have combined to

produce detailed information on the structure of phases. Since the x-ray scattering cross-section can be expressed in terms of the Fourier transform of the density–density correlation function, the location of the scattering peak in reciprocal space determines the spatial periodicity present, while the structure of the peak indicates the spatial extent of this periodicity.

The positional order of nematic liquid crystals is short-range, but anisotropic. That is, the x-ray scattering cross-section of an oriented monodomain sample shows two diffuse spots. One represents a wavevector $q_{\|} = 2\pi/L$ along the director, where $L$ is on the order of a molecular length, and the other represents a wavevector $q_{\perp} = 2\pi/d$ perpendicular to the director, where $d$ is on the order of a molecular width. This indicates that there are two correlation lengths for short-range positional order in nematics, $\xi_{\|}$ along the director, and $\xi_{\perp}$ perpendicular to the director. The diffuse spot along the director sometimes grows in intensity and sharpens as the temperature is lowered in the nematic phase and a smectic A phase is approached. This is a precursor to the ordering present in smectic layers, and exactly how this order builds up has been the focus of a great deal of both theoretical and experimental research. This will be discussed at length in a later section.

## 4.1.2 Chiral Nematic Liquid Crystals

### 4.1.2.1 Intrinsic Twist

Although the nematic phase is characterized by a director which does not vary spatially, there are many liquid crystals with spatially varying directors. Most of these involve twist, so a general description of twist in liquid crystals is required. Liquid crystal phases with intrinsic twist are possible whenever the molecules of the liquid crystal are chiral, that is, lack a center of inversion symmetry. While chiral liquid crystal molecules possess both chiral and achiral liquid crystal phases, no achiral molecules form chiral liquid crystal phases. Perhaps the most convenient formulation to describe the twist is through the variation of a macroscopic tensor property, such as the anisotropic part of the electric susceptibility, $\varepsilon_{ij}$.

Imagine a chiral nematic liquid crystal with a pitch $P$ and a helical axis directed along the $z$-axis. The components of the director $\hat{n}$ can be expressed quite easily:

$$n_x = \cos(2\pi z/P) \qquad n_y = \sin(2\pi z/P) \qquad n_z = 0. \quad (4.8)$$

The anisotropic part of the electric susceptibility is given by $\varepsilon_{ij} = \varepsilon_a(n_i n_j - \delta_{ij}/3)$ where $\varepsilon_a$ is the anisotropy or difference between the electric susceptibility parallel and perpendicular to the director, $\varepsilon_{\|} - \varepsilon_{\perp}$. This means that $\varepsilon_{ij}$ takes the following form:

$$\varepsilon_{ij} = \frac{\varepsilon_a}{3}\begin{pmatrix} \frac{1}{2}+\frac{3}{2}\cos\left(\frac{4\pi z}{P}\right) & \frac{3}{2}\sin\left(\frac{4\pi z}{P}\right) & 0 \\ \frac{3}{2}\sin\left(\frac{4\pi z}{P}\right) & \frac{1}{2}-\frac{3}{2}\cos\left(\frac{4\pi z}{P}\right) & 0 \\ 0 & 0 & -1 \end{pmatrix}. \quad (4.9)$$

It is important to see this expression for the anisotropic part of a tensor property for a chiral nematic liquid crystal as a specific example for a more general treatment of the problem. Since $\varepsilon_{ij}$ is a symmetric tensor with zero trace, five independent quantities are necessary to specify it in general. For chiral systems, the most convenient way to do this is to define five basis tensors, each isomorphic to the spherical harmonics of order two (Brazovskii and Dmitriev, 1975; and Brazovskii and Filev, 1978):

$$T_{ij}^{\pm 2} = \frac{1}{2}\begin{pmatrix} 1 & \pm i & 0 \\ \pm i & -1 & 0 \\ 0 & 0 & 0 \end{pmatrix}$$

$$T_{ij}^{\pm 1} = \frac{1}{2}\begin{pmatrix} 0 & 0 & 1 \\ 0 & 0 & \pm i \\ 1 & \pm i & 0 \end{pmatrix} \quad (4.10)$$

$$T_{ij}^{0} = \frac{1}{\sqrt{6}}\begin{pmatrix} -1 & 0 & 0 \\ 0 & -1 & 0 \\ 0 & 0 & 2 \end{pmatrix}.$$

The anisotropic part of the electric susceptibility can then be written in terms of the basis tensors,

$$\varepsilon_{ij} = \frac{1}{2}\sum_{m=-2}^{+2}\left(\varepsilon_m T_{ij}^{m}\, e^{i\vec{q}\cdot\vec{r}} + \varepsilon_m^{*} T_{ij}^{m^{*}}\, e^{-i\vec{q}\cdot\vec{r}}\right) \quad (4.11)$$

where $\varepsilon_m$ is the amplitude of the "structural mode" described by each basis tensor and $m = -2, -1, 0, +1, +2$ (Grebel et al., 1983, 1984). The $m = \pm 2$ modes describe a planar spiral variation of the director, with the $-2$ mode being right-handed and the $+2$ mode being left-handed. The $m = \pm 1$ modes describe a conical spiral variation of the director, with the principal

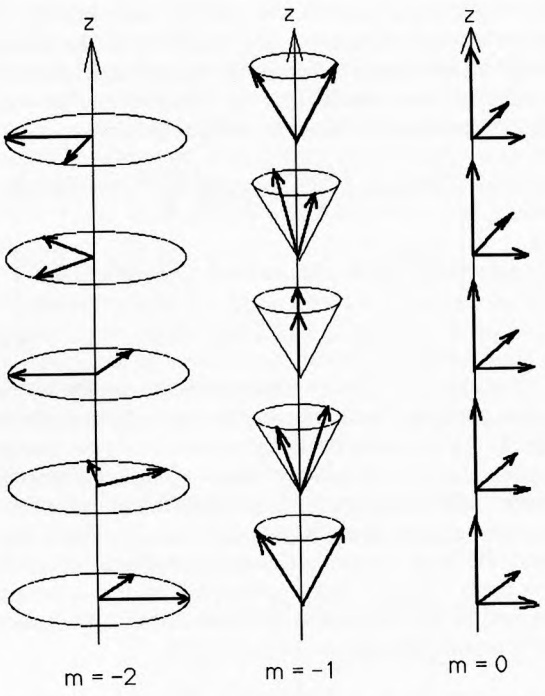


FIGURE 4.1. Three of the five structural "modes" useful in describing the orientational order in a chiral liquid crystal. The two additional "modes" are the $m = +2$ and $m = +1$ "modes," which are the left-handed analogs of the $m = -2$ and $m = -1$ "modes," respectively.

axes of the director making a constant angle of 45° to the helical axis. The $m = -1$ mode is right-handed and the $m = +1$ mode is left-handed. The $m = 0$ mode describes the achiral mode appropriate for a nematic liquid crystal. Using this formulation, $\varepsilon_{ij}$ for the chiral nematic liquid crystal described by (4.9) is just a combination of the $m = -2$ and $m = 0$ modes with $\varepsilon_m$ equal to $-\varepsilon_a/\sqrt{6}$ and $\varepsilon_a/2$, respectively, and with $q = 4\pi/P$. FIGURE 4.1 shows the principal axes for the $m = -2$, $-1$, and 0 structural modes.

While the smallest pitch encountered is about 100 nm (Yang and Crooker, 1987), there is no bound as to how long the pitch can be. In fact, mixing equal amounts of the stereoisomers produces a nematic phase, that is, a chiral nematic phase with an infinite pitch. The uniform variation in the refractive index due to the helical structure produces spectacular optical effects for light with a wavelength in the liquid crystal equal to the pitch. These include the reflection of circularly polarized light and anomalous optical activity (Chandrasekhar, 1992; and de Gennes and Prost, 1993). The fact that at normal incidence there are no higher order reflections indicates that the components of the director are well described by a sinusoidal function.

#### 4.1.2.2 Local Nematic Order

Since the pitch is at least ten times larger than a typical molecular width, a thin slice perpendicular to the helical axis several molecular widths wide possesses orientational order which is very similar to a nematic. For this reason, chiral nematic liquid crystals are described as twisted nematic phases. It should be kept in mind, however, that the uniaxial symmetry of the nematic phase is broken by the twist, that is, one direction perpendicular to the local director is parallel to the helical axis and the other orthogonal direction is perpendicular to the helical axis. Since the twist is usually small on a molecular scale, this is a very small effect in most cases.

There is at least one situation where the fact that a chiral nematic is not locally uniaxial does become important. When the coherence length for orientational fluctuations and the pitch become comparable, the biaxial character of the local orientational order is crucial and new phases become stable. These are the so-called blue phases and are discussed later in the chapter.

### 4.1.3 Smectic Liquid Crystals

#### 4.1.3.1 Positional Order

Short-range, quasi-long-range, and long-range positional order all occur in smectic liquid crystals. While the dominant positional order is a tendency to form a layered structure, positional order of various kinds can occur in the two directions parallel to the layers. Of course, when long-range order in all three directions is present, the phase is crystalline, but in many liquid crystalline materials a number of crystalline phases form in which the amount of disorder is quite high. These phases are characterized by only a small number of independent x-ray reflections, and large entropy and volume changes at the transition to the highly ordered crystal phase at lower temperatures.

The smectic A phase possesses positional order in one dimension, that is, there is a tendency for the

molecules to be in layers which have normals parallel to the director. De Gennes first represented this order as a sinusoidal variation in the density:

$$\rho(\vec{r}) = \bar{\rho} + \mathrm{Re}\{\Psi \cdot e^{i(2\pi/L)z}\}. \qquad (4.12)$$

Here $L$ is the spacing between the layers and $z$ is along the director. $\Psi$ is a complex order parameter: $|\Psi|$ is a measure of the change in density in going from layer to layer, and the phase of $\Psi$ describes where the layers are along the $z$-axis (de Gennes, 1972).

It has long been known that true long-range order in only one dimension is not possible (Peierls, 1934; and Landau, 1965). These arguments can be extended to liquid crystalline systems (Caille, 1972), where it is shown that the density–density correlation function decays as some power of the distance (quasi-long-range order). Experimental confirmation of this has been achieved in both thermotropic and lyotropic systems (Als-Nielsen et al., 1980; and Safinya et al., 1986). The positional order within the layers is short-range in smectic A liquid crystals, with correlation lengths of only a few molecular widths.

#### 4.1.3.2 Non-polar Smectics

Positional order in the plane perpendicular to the director can take many forms. In the hexatic smectic B phase, this positional order is quasi-long-range in the direction normal to the layers and short-range, but with much longer correlation lengths than in the smectic A phase, within the plane of the layers. The interesting additional feature is the presence of long-range bond orientational order within the layers. Bond orientational order implies that in spite of the fact that positional order within the layers is only short-range and is weakly correlated from layer to layer, the in-plane crystallographic axes are maintained over large distances both parallel and perpendicular to the layers. Locally the molecules are packed with hexagonal symmetry, and the orientation of the sixfold symmteric axes is maintained with true long-range order. The fact that a crystal with two-dimensional order can melt to a phase with hexatic order was first proposed by a number of workers (Halperin and Nelson, 1978; Nelson and Halperin, 1979; and Young, 1979). The reason for this is an instability against the spontaneous creation of dislocations, which produces short-range positional order but maintains long-range order in the orientation of the crystallographic axes.

With the presence of long-range positional order in the plane perpendicular to the director, disordered crystalline phases are formed. The crystal B phase is similar to the hexatic B phase, but now long-range positional order exists both within the layers and from layer to layer. While the molecular centers are packed with hexagonal symmetry within the layers, the molecules are free to rotate about the normal to the layers. This rotational freedom is frozen out in the crystal E phase, where the transverse axes of the four nearest neighbors are rotated by 90° relative to the transverse axes of the center molecule. All molecules undergo rapid rotations of 180° about their long axes. This results is what is called a herringbone pattern within the layers, and a lattice that has rectangular symmetry. Both the crystal B and E phases show sharp Bragg-like x-ray reflections, indicative of structures with long-range order (Leadbetter, 1987; and Pershan, 1988).

There are also versions of these phases in which the director is not normal to the layers, but tilted at an angle of up to 45°. The tilted analog of the smectic A phase is called the smectic C phase. In many cases the tilt angle increases from a very small value just below the smectic A to smectic C transition to a value typically around 30°. There is still short-range positional order within the planes. The hexatic smectic F and I phases are tilted versions of the hexatic smectic B phase. In the hexatic smectic F phase, the molecular tilt is toward the midpoint of the line connecting two nearest neighbors; in the hexatic smectic I phase, the molecular tilt is toward a nearest neighbor. Since these phases have long-range bond orientational order, the direction of tilt is maintained over large distances both within and perpendicular to the planes. The crystal G and K phases are the tilted analogs to the crystal B phase, with the tilt being toward the side of the hexagon in the crystal G phase, and toward the apex of the hexagon in the crystal J phase. The molecules in both phases rotate freely about their long molecular axes. Finally, the crystal H and K phases correspond to tilted versions of the crystal E phase. In the crystal H phase the tilt is toward a next nearest neighbor, like the crystal G phase. In the crystal K phase, the tilt is toward a nearest neighbor, like the crystal J phase. Rotation motion about the long molecular axis is restricted as in the crystal E phase (Leadbetter, 1987; and Pershan, 1988).

Finally, there are chiral versions of these tilted smectic and crystal phases. This occurs if the molecule

itself is chiral, that is, it lacks inversion symmetry. Such molecules can form smectic phases which are nonchiral, such as the smectic A phase, but tilted smectic phases of these molecules have a helical structure. If the normal to the smectic layers is the z-axis, then the director rotates about a cone from layer to layer. The generating angle of the cone is just the tilt angle of the smectic phase. The smallest pitch for a chiral smectic C phase (denoted smectic C*) is around 300 nm.

A chiral smectic C liquid crystal with a pitch of P and a helical axis in the z-direction has components of the director in all directions at some point in the structure:

$$n_x = \sin\theta\cos(2\pi z/P) \qquad n_y = \sin\theta\sin(2\pi z/P) \qquad n_z = \cos\theta \tag{4.13}$$

Therefore, $\varepsilon_{ij}$ takes the following form:

$$\varepsilon_a \begin{pmatrix} \sin^2\theta\cos^2\left(\frac{2\pi z}{P}\right) - \left(\frac{1}{3}\right) & \sin^2\theta\sin\left(\frac{2\pi z}{P}\right)\cos\left(\frac{2\pi z}{P}\right) & \sin\theta\cos\theta\cos\left(\frac{2\pi z}{P}\right) \\ \sin^2\theta\sin\left(\frac{2\pi z}{P}\right)\cos\left(\frac{2\pi z}{P}\right) & -\sin^2\theta\sin^2\left(\frac{2\pi z}{P}\right) - \left(\frac{1}{3}\right) & \sin\theta\cos\theta\sin\left(\frac{2\pi z}{P}\right) \\ \sin\theta\cos\theta\cos\left(\frac{2\pi z}{P}\right) & \sin\theta\cos\theta\sin\left(\frac{2\pi z}{P}\right) & \cos^2\theta - \left(\frac{1}{3}\right) \end{pmatrix} \tag{4.14}$$

As in the case of chiral nematics, $\varepsilon_{ij}$ can be expressed as a linear combination of the structural modes described by the tensor in (4.10). Three modes contribute and the amount of each depends on the tilt angle. For a right-handed helicoidal phase, the amount of $m = 0$ contribution is proportional to $(3\cos^2\theta - 1)/2$, the amount of $m = -1$ contribution is proportional to $\sin\theta\cos\theta$, and the amount of $m = -2$ contribution is proportional to $\sin^2\theta$, where $\theta$ is the tilt angle.

**Phases of Non-polar Molecules with Positional Order**

| Non-tilted | Tilted | Chiral | Positional Order: Between Planes | Positional Order: Within Planes | Bond Orientational Order |
|---|---|---|---|---|---|
| Smectic A | Smectic C | Smectic C* | S | S | S |
| Hexatic B | Smectic F,I | Sm. F*,I* | Q | S | L |
| Crystal B | Crys. G,J | Crys. G*,J* | L | L | L |
| Crystal E | Crys. H,K | Crys. H*,K* | L | L | L |

S = short-range order  Q = quasi-long-range order  L = long-range order

FIGURE 4.2. Chart of layered liquid crystal and "soft crystal" phases.

There are also antiferroelectric and ferrielectric forms of the chiral smectic C phase (Chandari et al., 1989; Gorecka et al., 1990; and Inui et al., 1990). In the antiferroelectric phase, even though the director rotates in helical fashion along the direction perpendicular to the layers, neighboring layers have in-layer projections of the director which are approximately in opposite directions. The electric polarization is in the plane of the layer, perpendicular to the director, and antiparallel in neighboring layers, producing an antiferroelectric phase. The ferrielectric phase is thought to be similar to the chiral smectic C antiferroelectric phase, but with unequal numbers of layers with polarization in opposite directions. This creates a phase with net electric polarization. These helicoidal phases are both scientifically and technologically important, and are discussed in Chapter 5.

FIGURE 4.2 summarizes the phases found in nonpolar liquid crystals along with the most important properties of each.

#### 4.1.3.3 Polar Smectics

The smectic phases formed by highly polar molecules or mixtures of highly polar molecules include some of the phases described for nonpolar molecules, but also include a number of additional phases. When a smectic A or smectic C phase is present with complete head-to-tail disorder within the layers, then these phases are called smectic $A_1$ or smectic $C_1$ if the molecules are polar. However, polar molecules also

form smectic A and C phases in which there is antiferroelectric ordering of pairs of layers. Since the spatial periodicity is two layers in these phases, they are called smectic $A_2$ and smectic $C_2$. In some systems, there is a good deal of molecular association of pairs of molecules (parallel long axes, partial overlap). A smectic phase with a periodicity of between one and two molecular lengths sometimes occurs in these compounds and is called the smectic $A_d$ or smectic $C_d$ phase, depending on the orientation of the director relative to the layer normal. Finally, a modulated phase occurs in some highly polar systems, in which antiferroelectric ordering of neighboring layers is modulated in two directions, one parallel to the director and the other perpendicular to the director. These are called the smectic $\tilde{A}$ and smectic $\tilde{C}$ phases or smectic A and C fluid antiphases. All of the smectic phases of polar molecules are sometimes referred to as frustrated smectic phases. This term stems from the fact that one periodicity is locked in for each phase; the other periodicities are frustrated and are absent.

These phases are usually identified from x-ray scattering experiments. The smectic $A_1$ phase produces an on-axis quasi-Bragg peak at a reciprocal wavevector of $2\pi/L$, where $L$ is on the order of a molecular length. The x-ray pattern for the smectic $A_2$ phase shows a reciprocal wavevector at $\pi/L$, while the smectic $A_d$ phase has a peak at $2\pi/L'$, where $L'$ is between $L$ and $2L$. All these peaks are on-axis. The smectic $\tilde{A}$ phase shows weak, diffuse off-axis peaks. In fact, these spots can be seen in the smectic $A_1$ phase, near the transition to the smectic $\tilde{A}$ phase (Young et al., 1994). The smectic C phases corresponding to these A phases have similar x-ray reflections, but the tilt of the director relative to the layer normal shifts the peaks off-axis.

X-ray measurements on these highly polar smectic systems have also revealed that phases with more than one periodicity may occur. In the smectic $A_{inc}$ phase (inc = incommensurate), peaks indicating both $A_d$ and $A_2$ ordering are present (Ratna et al., 1985). Likewise, the smectic $A_{cren}$ phase (cren = crenelated) shows peaks indicating a modulation of the antiferroelectric order as in the smectic $\tilde{A}$ phase, but with regions of opposite polarization not equal in size (Levelut, 1984). The existence of both of these phases is doubtful, as revealed by recent experiments which showed that these phases are probably broad two-phase regions due to extremely slow conversion of one phase to the other (Kumar et al., 1991; Patel et al., 1992; and Young et al., 1994). For example, following a change in temperature across a phase transition in a mixture of a nonpolar and polar liquid crystal, x-ray peak intensities changed with a time constant of about half a day.

A phenomenological theory is useful in understanding the existence of these phases in polar smectic liquid crystals (Prost, 1984; Wang and Lubensky, 1984; and Lubensky et al., 1988). In this theory, two order parameters are used to describe the tendency of the molecules to form layers. The first is the normal smectic order parameter describing the amplitude of the mass density wave. The second is the amplitude of a wave describing the antiparallel association of either molecules or layers. While the first order parameter is associated with a wavevector equal to $2\pi/L$, where $L$ is a molecular length, the second order parameter is associated with a wavevector equal to $2\pi/L'$, where $L'$ is between one and two molecular lengths. Terms in the free energy which include both order parameters compete with the elastic energy and produce several phases: the $A_1$ phase with only the first order parameter nonzero; the $A_2$ phase with both order parameters about equal; and the $A_d$ phase with the second order parameter significantly greater than the first. This theory also predicts that smectic phases with incommensurate wavevectors are possible when the mismatch between the two wavevectors is great.

One other property of polar smectics is the existence of reentrant phases. First discovered in a mixture of two polar compounds, cooling the sample resulted in the phase sequence isotropic–nematic–smectic $A_d$–nematic–solid (Cladis, 1975). The most extreme example of reentrant behavior is probably the compound 4-nonyloxyphenyl-4′-nitrobenzoyloxybenzoate, which has the following phase sequence on cooling: iso–N–$A_d$–N–$A_d$–N–$A_1$–$\tilde{C}$–$A_2$–$C_2$–solid (Tinh et al., 1982). Such behavior can be understood both in terms of mean-field theory if certain coefficients have appropriate temperature and pressure dependences (Prost, 1979) and by packing considerations for molecules with a tendency for antiparallel pairing (Cladis, 1980).

One final phase which is worthy of note is the "smectic D" phase, first discovered in a laterally substituted carboxylic acid compound. This phase is optically isotropic and occurs between the smectic C and smectic A phases or between the smectic C and

isotropic phases. Recent x-ray measurements have shown that it is a three-dimensional cubic crystal, with a unit cell of about 800 molecules. A second type of "cubic smectic" phase has also been found in nonsubstituted, nonpolar liquid crystals. This phase exists between the crystal and smectic C phase and seems to have a unit cell about half the size of the first "smectic D" phase described. Clearly these phases possess three-dimensional order and should be referred to as crystals rather than smectic phases (Leadbetter, 1987; and Pershan, 1988).

#### 4.1.3.4 Mixture and Pressure Studies

The study of mixtures has been an important component of research into smectic phases. Typically, various concentrations of two compounds are prepared and the phases present as a function of temperature are determined. This results in a phase diagram for the mixture. If a phase of each pure compound is connected across the phase diagram, then that is good evidence that the phases in each pure compound are in fact the same. Much more important, however, is the fact that firstly, "induced phases" are sometimes present for some concentration range of the mixture when that phase does not exist in either of the pure compounds, and secondly, phase boundaries in the mixtures show interesting topologies when either the two pure compounds possess different phase sequences, or induced phases are present. Much of the work on reentrant phases has been done in mixtures, and mixtures of polar and nonpolar smectic liquid crystals have provided a wealth of information on the polymorphism in smectic liquid crystals. A good example of the polymorphism in a binary mixture is shown in FIGURE 4.3, where four different smectic phases are present, with one of them occuring in two regions (Levelut et al., 1981).

Pressure studies have also been important in understanding smectic phases. Because high-pressure experiments are much more difficult than mixture experiments, many fewer of them have been performed. One of the important consequences of these pressure experiments has been to confirm many of the findings coming out of experiments on mixtures. While pressure is a true thermodynamic variable which can be changed for a system of a single composition, the concentration in a mixture experiment suffers from the fact that the actual system being studied changes as the concentration is varied. When the behavior of a single compound under presssure corresponds to the behavior of a mixture as the concentration is changed, there is reason to have some faith that the behavior can be explained in simple terms. A good example of this is the pressure experiment on the reentrant behavior of a single polar compound that compared favorably with the experiments on mixtures of two similar polar compounds (Cladis et al., 1977).

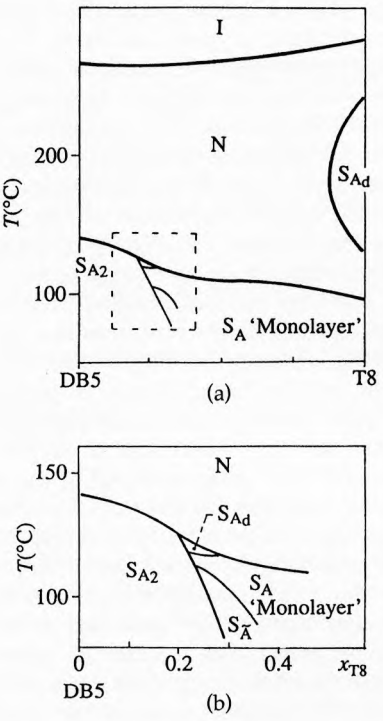


FIGURE 4.3. Polymorphism in a binary mixture of two liquid crystals. The entire phase diagram is shown in (a) and an enlarged inset is shown in (b). (From Levelut et al., 1981.)

### 4.1.4 Defect Phases

#### 4.1.4.1 Blues Phases

While chiral nematics can be viewed as slightly twisted nematics in systems where the chirality is low (and the pitch is long), such is not the case for highly chiral systems. The presence of a large additional term in the free energy promotes the formation

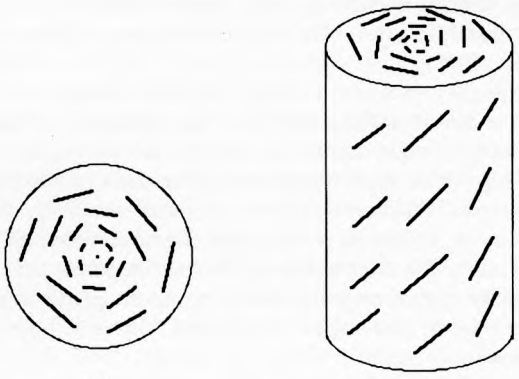


FIGURE 4.4. Double twist cylinder, in which the director rotates by 45° in all directions radial to the central axis. (a) Top view; (b) side view.

of a double twist structure rather than the single twist structure typical of the chiral nematic phase. In the double twist structure, the director rotates about every axis in a plane as shown in FIGURE 4.4(a). The free energy of such a structure is lower than the free energy of the chiral nematic structure only near the center. This means that macroscopic phases with double twist must be comprised of many of these structures. For example, if the double twist structure ends when the director is rotated by 45°, then a macroscopic phase can be made from many of these double twist cylinders (see FIGURE 4.4(b)). Although such double twist cylinders which meet at right angles can have a continuous rotation of the director in going from one cylinder to the next, the points in the region between three orthogonal double twist cylinders possess a defect where the orientational order goes to zero and the director is undefined. Examples of a simple cubic structure and a body centered structure composed of double twist cylinders are shown in FIGURES 4.5(a) and (b), respectively. The defects in both structures are line defects in which the director rotates by 180° in going around the defect. The lattice constant for these structures is roughly one half the pitch. One can also imagine a random assortment of double twist cylinders, with an accompanying arrangement of line defects typical of an amorphous phase. As has been pointed out, chiral structures are inherently biaxial, although the biaxiality in chiral nematics is very small and of little importance. Such is not the case for the

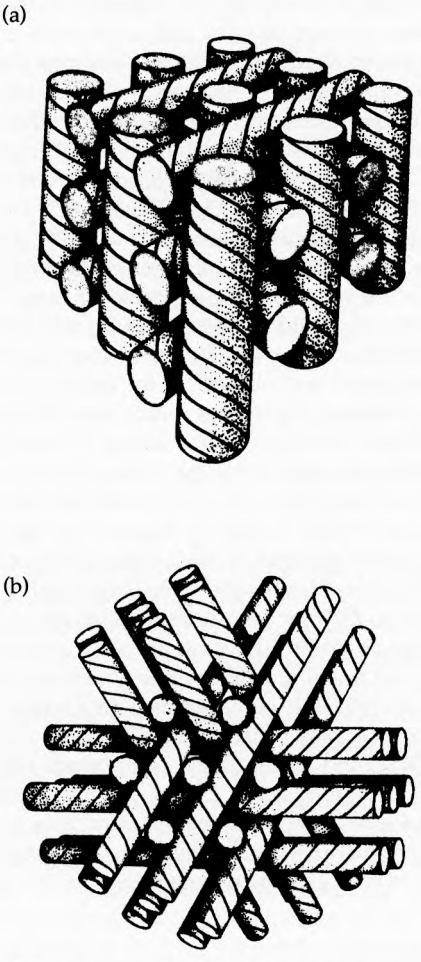


FIGURE 4.5. Two possible defect phases composed of double twist cylinders. (a) a simple cubic structure; (b) a body centered cubic structure. (From Grebel et al., 1984.)

phases of highly chiral substances made from double twist cylinders.

These three structures (simple cubic, body centered cubic, and amorphous) exist in chiral liquid crystals if the pitch is small. Usually they are stable in a very narrow temperature region (on the order of 1 K) between the chiral nematic and isotropic phases. These phases are called the blue phases, because they were first discovered in materials which reflected ultraviolet light in the chiral nematic phase and blue light in the phases with cubic symmetry. The color of

reflected light is determined by the pitch of the structure in exact analogy to x-ray diffraction from crystals, so blue phases which reflect at wavelengths throughout the visible spectrum have been observed. Several recent reviews excellently summarize the theoretical and experimental work on blue phases (Wright and Mermin, 1989; Crooker, 1989; Hornreich and Shtrikman, 1989; Seideman, 1990; and Keyes, 1991).

A useful way to view the stability of the blue phases is through experiments on mixtures of the two optical isomers of the same chiral compound. In some senses these mixtures should be thermodynamically identical except for the pitch, which is a minimum for either of the pure isomers and infinite for the racemic mixture. FIGURE 4.6 shows the phases which are stable as the chiral fraction (amount of pure isomer divided by the sum of the amounts of pure isomer and racemic mixture) is increased from zero to one for one particular liquid crystal. Notice (1) that at a certain chiral fraction, the body centered cubic phase (BPI) forms; (2) that at a higher chiral fraction, the simple cubic phase (BPII) forms; (3) that at a higher chiral fraction, the amphorous phase (BPIII) forms; and (4) that at an even higher chiral fraction, BPII becomes unstable, leaving only BPI and BPIII. In compounds with a longer pitch, the pure isomer may possess only BPI, or BPI and BPII, or BPI, BPII, and BPIII. These compounds therefore represent a region of the phase diagram shown in FIGURE 4.6 extending from the left-hand axis to some point in the middle of the diagram. All compounds which have been investigated to date, however, follow this scheme of BPI first, BPII second, BPIII third, and loss of BPII as the chiral fraction is increased (Bowling et al., 1993).

Single crystals of a blue phase with dimensions on the order of millimeters have been grown, and thus there have been numerous experiments performed on both powder samples and single crystals in addition to optical diffraction. Facets on these single crystals are even visible in some cases. Optical microscopy, including the observation of Kossel diagrams, optical activity measurements, and nuclear magnetic resonance experiments have been used to probe the blue phases.

### 4.1.4.2 Twist Grain Boundary Phases

Chirality is responsible for a slightly different phenomenon in smectic liquid crystals. Because of the layered structure, smectic liquid crystals do not allow for twist, so in many cases chiral molecules possess the nonchiral smectic A phase. However, in compounds with a very short pitch, the free energy of the phase is lowered by introducing twist grain boundaries at regular intervals. The phase is therefore a succession of undistorted smectic blocks, separated at regular intervals by defect or fluid-like regions where the layer structure and director rotate by a small angle. This structure is shown in FIGURE 4.7, where it can be seen that the twist axis is in the plane of the layers with the director perpendicular to this twist axis. In one compound, a rotation of the smectic blocks by $\Delta\Psi = 17°$ occurs at twist grain boundaries spaced $l_b = 24\,\text{nm}$ apart. This results in a pitch of about

FIGURE 4.6. Temperature–chirality phase diagram. (From Bowling et al., 1993.)

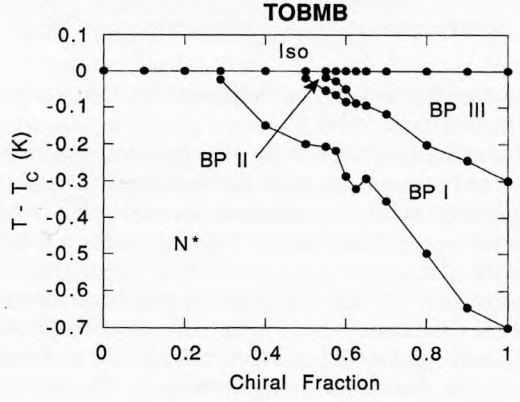


FIGURE 4.7. Twist grain boundary (TGB) phase. (Reprinted with permission from Ihn et al., *Science* 258, 1992. Copyright American Association for the Advancement of Science.)

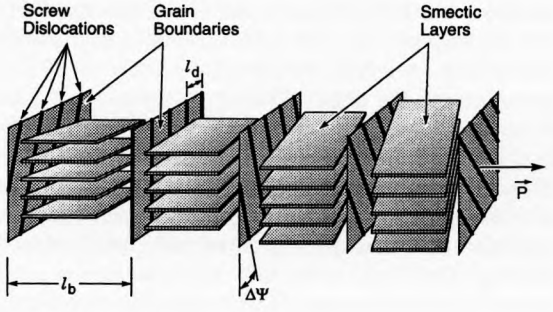

500 nm and a resulting optical reflection of about 800 nm (Ihn et al., 1992). Such a twist grain boundary A phase (TGB A phase) was theoretically predicted (Renn and Lubensky, 1988) and experimentally observed (Goodby et al., 1989) at about the same time. Since that time there has been both additional theoretical (Renn, 1992) and experimental (Navailles et al., 1993) work on the twist grain boundary C phase (TGB C) in addition to the TGB A phase.

This work on the twist grain boundary phases has extended the analogy between superconductors and smectic A liquid crystals first pointed out by de Gennes. Both possess a complex order parameter and a free energy of the same form (de Gennes, 1972). Twist distortion in smectic A liquid crystals plays the same role as the magnetic field for superconductors. Type-I superconductors expel the magnetic field just as smectic A liquid crystals possess no twist distortion, even when the molecules are chiral. Type-II superconductors allow the magnetic field to penetrate in flux vortices just as the TGB A phase incorporates twist in grain boundaries. The TGB A phase, with its regular spaced array of twist grain boundaries, is analogous to the lattice of flux vortices of the Abrikosov phase in superconductors.

## 4.1.5 Discotic Liquid Crystals

### 4.1.5.1 Nematic Phase

One of the most important findings of the last fifteen years is that disk-shaped molecules can form liquid crystal phases (Chandrasekhar and Ranganath, 1990). These molecules are called discotic liquid crystals and usually possess a flat core connected to four, six, or eight long chains via ester or ether linkages. FIGURE 4.8 shows a molecule with two discotic phases. X-ray scattering and NMR spectroscopy experiments show that the cores are well ordered and the chains are not; yet the chains seem to be crucial to the stability of these phases.

The most simple discotic phase is the nematic phase, sometimes given the notiation $N_D$, so as not to confuse it with the nematic phase of rod-like molecules. As shown in FIGURE 4.9(a), it is the short axes of the molecules which preferentially orient along the director. There is no long-range positional order. While the symmetry of the nematic phases for both rod-like and disk-like molecules is the same, the nematic phase of rod-like molecules is diamagnetically

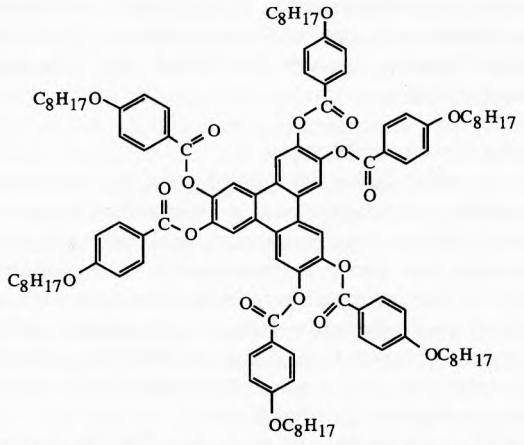


FIGURE 4.8. Discotic liquid crystal possessing both columnar and nematic phases.

and optically positive while the nematic phase of disk-like molecules is negative. The dielectric anisotropy of both nematic phases can be either positive or negative.

Nematic phases occur in compounds with shorter chains. In fact, lengthening the chains in a homologous series narrows the nematic phase and eventually eliminates it, just as for the nematic phase of rod-like molecules. There has not been a great deal of work done on the $N_D$ phase, but what has been done reveals that the elastic constants for disk-like and rod-like systems are similar, and the viscosity of the disk-like systems is much higher (Chandrasekhar, 1992). A chiral nematic phase has been observed in discotic systems, with the director perpendicular to the helical axis, just as in the chiral nematic phase of rod-like

FIGURE 4.9. Structure of the nematic (a) and columnar (b) phases.

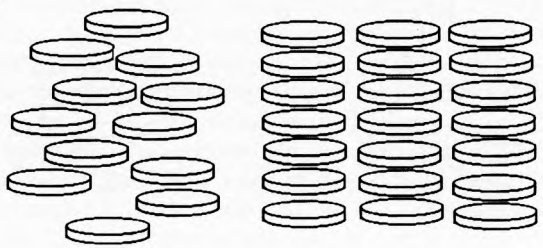

(a) (b)

molecules (Destrade et al., 1980). Finally, a reentrant $N_D$ phase exists between two columnar phases of certain truxene derivatives (Frank and Chandrasekhar, 1980).

#### 4.1.5.2 Columnar Phase

FIGURE 4.9(b) shows the type of positional order present in the columnar phases of discotic liquid crystals. There is still no long-range positional order along the columns, but there is two-dimensional positional order of the columns themselves. The columns can either form a rectangular lattice or a hexagonal lattice. Along the columns, long-range orientational order of the molecular cores is present, but the flexible chains are again highly disordered.

In the rectangular columnar phase $D_r$, the columns occupy a rectangular lattice but the short axis of the molecules in each column is tilted away from the column axis. The tilt direction of the columns is a herringbone arrangement as shown in FIGURE 4.10(a). The higher-temperature hexagonal columnar phase $D_h$ possesses a hexagonal lattice of columns with the molecules tilted within the columns, but there is no order in the azimuthal direction of the tilt. This arrangement is shown in FIGURE 4.10(b).

There is also evidence for phases in which the positional order of the molecules along the column is long-range in addition to the two-dimensional order of the columns themselves. Since true long-range positional order in one dimension is forbidden by the Landau–Peierls instability, there must be ordering between the molecules in neighboring columns. Experiments with freely suspended strands of these ordered phases reveal a helicoidal stacking of the molecular cores and triangular superlattice (Fontes et al., 1988). These "ordered" discotic phases obviously have much in common with the three-dimensionally ordered smectic phases, and therefore should be referred to as soft crystals rather than liquid crystals.

FIGURE 4.10. The rectangular (a) and hexagonal (b) columnar phases. The molecules are tiled with respect to the column axis in both phases.

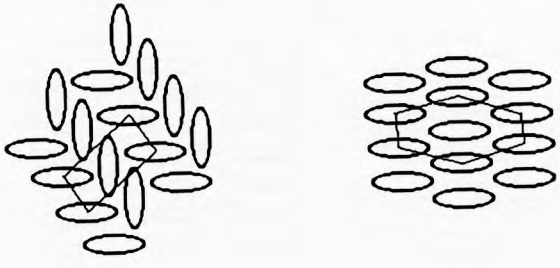

(a) (b)

#### 4.1.5.3 Biaxial Nematic Phase

The existence of a biaxial nematic phase has been the subject of discussion for a long time. In such a phase, the molecular axes perpendicular to the long axis of a rod-shaped molecule possess long-range orientational order just as the long molecular axis does. The most common example is a fluid of orthorhombic molecules, in which each molecular axis defines three orthogonal directors. Such a phase was first discovered in a lyotropic system, where for certain concentration and temperature conditions, the micelles did not possess cylindrical symmetry (Yu and Saupe, 1980).

The first thermotropic biaxial nematic phases were seen in molecules containing both rod-like and disk-like features. In one case, the molecular core was a metal complex with four attached groups: two long rod-like groups at opposite ends and two small side groups perpendicular to the long axis of the molecule (Chandrasekhar et al., 1986). In another case, two disk-like groups with a benzene core were tethered together to form a long molecule (Praefcke et al., 1990). Both optical and x-ray experiments were used to ascertain that the molecular order was indeed biaxial.

### 4.1.6 Free Standing Films

#### 4.1.6.1 Smectic Films

A technique whereby free-standing films of smectic liquid crystal material can be made has been recently revived in an effort to study the transition from three-dimensional systems to two-dimensional systems. In this technique, some smectic material is drawn across a hole in a thin piece of glass or metal using the edge of another piece of glass or metal. The size of the hole is on the order of a few millimeters. By adjusting the amount of material, the speed at which it is drawn over the hole, and the temperature, free-standing smectic films of varying thicknesses (from a few layers up to thousands of layers) can be fashioned.

The smectic film is quite stable with the smectic layers in the plane of the film, and experiments can be performed on it for hours. The angular spread of the normal to the layers is extremely low in these films (on the order of a tenth to a hundredth of a degree compared with about one degree for a bulk liquid crystal aligned by a magnetic field). The majority of experiments on smectic films have been x-ray diffraction experiments probing the positional and orientation order within the film. Polarized light microscopy, light reflection spectroscopy, and heat capacity experiments have also been performed.

The stability of the smectic film is due to the energy barrier necessary to create a hole. The energy required to create a hole has two contributions: (1) the positive energy required to create an air–liquid crystal interface line, and (2) the negative energy from the decrease in the air–liquid crystal interface area. Since the first is proportional to the radius of the hole, while the second is proportional to the radius squared, the positive contribution wins for small radii. However, once a hole is created, it grows and the film pops (de Gennes and Prost, 1993).

In many cases, free-standing smectic films provide the ordered material which allows the various types of positional and orientational order in smectic liquid crystals to be understood (Moncton and Pindak, 1979; and Pindak et al., 1981). But thin films can have smectic phases not found in the bulk. For example, in one material in which the bulk possesses only crystal G and B phases, thin films show two additional crystal B phases and two tilted hexatic phases (Sirota et al., 1987).

In tilted smectic films of only a few layers, line defects where the orientation changes by multiples of $\pi/2$ have recently been studied. These lines form closed loops or terminate in fractional vortices and can be found in smectic C, hexatic smectic F, hexatic smectic I, and antiferroelectric phases (Pang et al., 1992).

#### 4.1.6.2 Surface Ordering

Free-standing films have also provided the means for a good deal of work probing the ordering that takes place near surfaces (in this case, the air–liquid crystal surface). For example, the liquid crystal 750BC has the following phase sequence upon cooling in the bulk: smectic A (65 °C)–hexatic B (59 °C)–crystal E. Yet in a ten-layer free-standing film of this material, the two outermost layers undergo a transition to the hexatic B phase at 71 °C, the next two outermost layers transform at 65.2 °C, followed by the bulk at 64.6 °C. Likewise, the two outermost layers transform to the crystal E phase at a higher temperature than the internal layers. This crystal E ordering of the two outermost layers also dramatically affects the hexatic B–smectic A transition for the inner layers (Geer et al., 1992).

Surface ordering has also been studied in bulk materials with an air–liquid crystal interface. An example is the smectic A ordering at the air–liquid crystal interface that occurs in nematic liquid crystals (Chen et al., 1989). Thin nematic films on an isotropic liquid substrate have also been used recently to study both the defects in these films (Lavrentovich and Nastishin, 1990) and the so-called "surface" elastic energy terms (Lavrentovich, 1991).

#### 4.1.6.3 Columnar Strands

When discotic material in a columar phase is spread across a hole, freely suspended strands form. The strands are typically tens of microns thick, meaning that they contain on the order of a thousand molecular columns. High-resolution x-ray experiments have revealed that the column axes are very well ordered (less than 0.3° variation on average) even though the strand contains several domains. The number of domains can be decreased by proper annealing of the strands (de Gennes and Prost, 1993).

## 4.2 PHASE TRANSITIONS

### 4.2.1 Universality Classes

One reason for the continued interest in liquid crystal phase transitions is that these transitions provide numerous examples for much of the recent theoretical work on critical phenomena. Because liquid crystal transitions are either weakly discontinuous or continuous, they should display the behavior associated with critical points, including strong fluctuations and diverging susceptibilities. One of the most important results of this theoretical work is that near such a transition, the microscopic details of the system become unimportant in describing how the transition takes place. Instead, the range of the interactions, the physical dimension of the system, and symmetry of the order parameter determine how the system behaves very close to the transition.

| Model | Order Parameter Symmetry | $\alpha$ | $\beta$ | $\gamma$ | $\nu$ |
|---|---|---|---|---|---|
| 2D Ising | scalar | 0 | 0.125 | 1.75 | 1 |
| 3D Ising | scalar | 0.1 | 0.33 | 1.24 | 0.63 |
| 3D XY | 2D vector | 0.01 | 0.34 | 1.30 | 0.66 |
| 3D Heisenberg | 3D vector | -0.12 | 0.36 | 1.39 | 0.71 |
| 2D Potts | scalar | 0.33 | 0.111 | 1.44 | 0.83 |

FIGURE 4.11. Some models for phase transitions.

The striking implication of this is that phase transitions in very different systems, superconductors and liquid crystals for example, may behave identically if the interactions, physical dimension, and symmetry of the order parameter are the same. To provide predictions, theorists have developed models of systems in which they can calculate the important thermodynamic properties. By convention these models are for magnetic systems, but they really correspond to a general interacting system with a particular type of interaction, dimension, and order-parameter symmetry. Some of these models, along with their dimensions and order-parameter symmetries, are described in FIGURE 4.11.

One parameter which is extremely important in describing the physical behavior near a phase transition is a critical exponent. This parameter gives the functional form of the divergence of a particular property. For example, the critical exponent $\alpha$ describes how the specific heat at constant magnetic field, $C_H$, diverges as the transition is approached by changing the temperature

$$C_H \propto |t|^{-\alpha} \tag{4.15}$$

where $t = (T - T_C)/T_C$ is the reduced temperature and $T_C$ is the transition temperature. This critical exponent is determined experimentally from the slope of a log–log plot of $C_H$ versus $t$,

$$\alpha = -\lim_{t \to 0} \left[ \frac{\ln(C_H)}{\ln(t)} \right]. \tag{4.16}$$

Other critical exponents describe the temperature variation of the order parameter ($\beta$), the susceptibility ($\gamma$), correlation length ($\nu$), etc. Values for the critical exponents from experiments are then compared with those predicted by the various models, to see how well the transition is described by the model. Some of these exponents for the various models are also given in FIGURE 4.11.

## 4.2.2 Liquid Crystal–Isotropic Transition

### 4.2.2.1 Nematic–Isotropic Transition

The transition from the nematic phase to the isotropic phase is always a discontinuous one, with a latent heat typically about $0.5\,\mathrm{kJ\,mol^{-1}}$, which is nearly two orders of magnitude smaller than for the melting of a solid to either the liquid crystal or the isotropic liquid phase. Due to the smallness of the latent heat, there are pretransitional effects on either side of the transtion. Values for the critical exponent $\alpha$ range from 0.3 and 0.4, depending on the range of temperatures used for the fit, while the critical exponent $\beta$ is around 0.25 (Thoen, 1992). These exponents are closer to those of a classical tricritical point ($\alpha = 0.5$ and $\beta = 0.25$), than those of mean-field theory ($\alpha = 0$ and $\beta = 0.5$). In general, the latent heat of the transition increases in a homologous series as the smectic–nematic transition gets closer to the nematic–isotropic transition.

The nematic–isotropic transition is usually described by the mean-field theory of Maier and Saupe or the phenomenological theory of Landau and de Gennes. In the latter, the free energy is expanded in powers of the order parameter

$$F = F_0 + \tfrac{1}{2}AS_{\alpha\beta}S_{\beta\alpha} + \tfrac{1}{3}BS_{\alpha\beta}S_{\beta\gamma}S_{\gamma\alpha} + \tfrac{1}{4}C(S_{\alpha\beta}S_{\beta\alpha})^2. \tag{4.17}$$

The constants B and C are greater than zero and $A = A_0(T - T^*)$, where $A_0$ is a constant. $F_0$ is the free energy of the isotropic phase. Since the transition occurs near where $A = 0$, $T^*$ sets the temperature of the transition. At temperatures well above $T^*$, the isotropic phase with $S_{\alpha\beta} = 0$ is stable. Below a temperature slightly above $T^*$, the nematic phase with $S_{\alpha\beta} \neq 0$ is stable. The presence of the cubic term insures that the transition will be discontinuous with both critical exponents $\alpha$ and $\beta$ equal to 0.5. As shown in FIGURE 4.12, enthalpy data show the discontinuous nature of the transition. Due to the smallness of the discontinuity, critical-like pretransition effects are present, but the values for critical exponents tend to depend on the range of temperature used for the fit.

A similar phenomenological theory is used to describe the short-range nematic order that is present in the isotropic phase just above the transition. The free

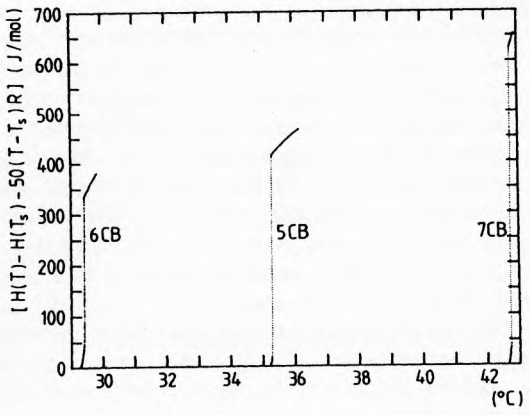


FIGURE 4.12. Enthalpy in the vicinity of the nematic–isotropic transition for three alkylcyanobiphenyls (nCB). (From Thoen et al., 1992.)

energy is expanded in terms of the order parameter and the spatial variation of the order parameter

$$F = F_0 + \tfrac{1}{2}AS_{\alpha\beta}S_{\beta\alpha} + \tfrac{1}{2}L_1\left(\frac{\partial S_{\beta\gamma}}{\partial x_\alpha}\right)\left(\frac{\partial S_{\beta\gamma}}{\partial x_\alpha}\right) + \tfrac{1}{2}L_2\left(\frac{\partial S_{\alpha\gamma}}{\partial x_\alpha}\right)\left(\frac{\partial S_{\beta\gamma}}{\partial x_\beta}\right). \tag{4.18}$$

$A = A_0(T - T^*)$ as before and $L_1$ and $L_2$ are constants. By expressing this free energy in terms of the Fourier transform of $S_{\alpha\beta}$ and then applying the equipartition theorem, the mean-square order parameter value in the isotropic phase varies with temperature as $(T - T^*)^{-1}$. This temperature dependence has been verified by light scattering experiments (Litster and Stinson, 1972), although it may break down close to the transition if a smectic phase exists below a narrow nematic phase (Gohin et al., 1983 and Anisimov et al., 1987).

#### 4.2.2.2 Blue Phase–Isotropic Transition

For chiral substances, the transition from the liquid crystal to isotropic phase can be from the chiral nematic, BPI, BPII, or BPIII phase to the isotropic liquid. The phenomenological Landau–de Gennes theory predicts that these transitions may be weaker than for nonchiral phases. The free energy for a chiral system has the following additional gradient term allowed by symmetry

$$\varepsilon_{\alpha\gamma\beta}S_{\alpha\beta}\left(\frac{\partial S_{\delta\beta}}{\partial x_\gamma}\right) \tag{4.19}$$

where $\varepsilon_{\alpha\gamma\delta}$ is the totally antisymmetric third rank tensor. It is convenient to express the free energy in terms of the Fourier transform of the order parameter and utilize the five basis tensors described previously. Then the free energy becomes

$$F = F_0 + \frac{1}{2}\sum_m \left\{A - mBq_0q + \left[B + \left(\frac{C}{6}\right)(4 - m^2)q^2\right]\right\}|S_m(q)|^2 \tag{4.20}$$

where $q_0 = 4\pi/P$ and $P$ is the pitch. The parameter $A$ has the same temperature dependence as before, while $B$ and $C$ are constants (Grebel et al., 1983, 1984). The effect of the new term is to shift the temperature dependence of the orientational order fluctuations in the isotropic phase for four of the structural modes. For the two modes with the same handedness as the liquid crystal phases, $T^*$ is shifted to higher temperature, and thus closer to the actual transition temperature. This has the effect of making the transition less discontinuous. This shift is proportional to $q_0^2$, so this effect should be strongest for the most chiral substances.

The blue phase to isotropic transition has been studied using heat capacity, optical activity, and light scattering measurements (Thoen, 1992; and Collings, 1992). For all but one of the compounds studied, all transitions between the chiral nematic and blue phases, between the blue phases themselves, and between the blue phases and the isotropic phase are first-order, although some have latent heats which are almost two orders of magnitude smaller than is typical for transitions from liquid crystals to the isotropic phase. The effect of increasing chirality on the transition to the isotropic phase is quite dramatic, as evidenced from the adiabatic scanning calorimetry on two systems in which the concentration of optical isomers was varied to change the chirality without affecting other physical parameters of the system (Voets, 1992; and Voets and Van Dael, 1993). For one compound, the latent heat of the BPIII–isotropic transition decreased from $1627\,\mathrm{mJ\,g^{-1}}$ in the racemic mixture to $785\,\mathrm{mJ\,g^{-1}}$ for the pure optical isomer. For another compound, this decrease was from $957\,\mathrm{mJ\,g^{-1}}$ to $147\,\mathrm{mJ\,g^{-1}}$. Very recent heat capacity and dynamic light scattering measurements on one of the most chiral compounds available indicates that the BPIII–isotropic transition is actually a supercritical

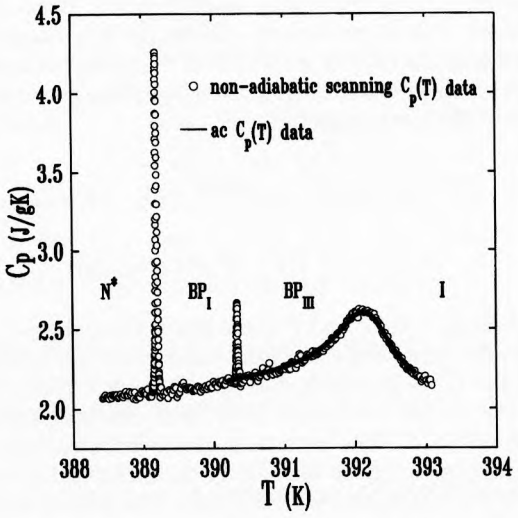


FIGURE 4.13. Specific heat in the chiral nematic phase (N*), first blue phase (BPI), third blue phase (BPIII), and isotropic phase (I) for a highly chiral liquid crystal. The N*–BPI and BPI–BPIII transitions are weakly first-order, while BPIII converts to I without a phase transition. (From Kutnjak et al., 1995.)

conversion and not a phase transition at all (Kutnjak et al., 1995). This is shown in FIGURE 4.13 where the latent heats for the chiral nematic–blue phase I and blue phase I–blue phase III transitions are clearly evident, but the blue III–isotropic transition region shows only a rounded conversion without a phase transition. The most important implication of this finding is that the macroscopic symmetry of the BPIII and isotropic phases must be the same.

#### 4.2.2.3 Smectic–Isotropic Transition

The latent heat for a direct transition from the smectic phase to the isotropic phase is considerably larger than for the nematic–isotropic transition (Thoen, 1992). Pretransitional effects, which include both orientational order and positional order fluctuations are less pronounced.

### 4.2.3 Smectic A–Nematic Transition

#### 4.2.3.1 Heat Capacity and X-ray Experiments

The transition from the smectic A phase to the nematic phase involves the melting of one-dimensional translational order. For the past two decades, this transition has received more theoretical and experimental attention than any other, partially due to the analogy with the superconducting–normal transition. Most of the focus has been on the critical exponents, in the hope of determining the universality class of this transition. In spite of all this research, the situation remains very complicated with numerous questions unresolved. A list of references to much of the theoretical and experimenal work is contained in a recent article (Garland and Nounesis, 1994).

The critical exponents that have been measured most extensively are $\alpha$, $\gamma$, $\nu_{||}$, and $\nu_{\perp}$, where the last two correspond to the divergence of the correlation lengths parallel and perpendicular to the director, respectively. In summarizing the data, it is convenient to specify the McMillan ratio, $T_{NA}/T_{NI}$, where $T_{NA}$ is the nematic–smectic A transition temperature and $T_{NI}$ is the nematic–isotropic transition temperature (McMillan, 1973). At first, differential scanning calorimetry (DSC) seemed to indicate that most of the observed smectic A–nematic transitions were discontinuous, with only those below the tricritical value of 0.87 being continuous, as suggested by McMillan. Later work utilizing adiabatic scanning calorimetry and AC calorimetry showed that pretransitional effects had been interpreted as latent heats in the DSC experiments, and that continuous behavior occurred up to much higher values of the McMillan ratio (Kasting et al., 1980; and Thoen et al., 1984). Experimental advances continue to be made in detecting small latent heats; a good example is the dynamical method using propagation characteristics of the interface between two phases (Cladis et al., 1989; and Anisimov et al., 1990).

The critical exponents for the susceptibility and correlation lengths are measured from diffuse x-ray scattering experiments in the nematic phase (Ocko et al., 1984). First, the x-ray structure factor is fit to the following form

$$\frac{\chi}{1+\xi_{||}^2 q_z^2+\xi_{\perp}^2 q_{\perp}^2(1+C\xi_{\perp}^2 q_{\perp}^2)} \tag{4.21}$$

where $C$ is a constant. Then the temperature dependences of $\chi$, $\xi_{||}$, and $\xi_{\perp}$ are fit to power laws to determine the critical exponents $\gamma$, $\nu_{||}$, and $\nu_{\perp}$, respectively. The power laws typically hold over three decades in reduced temperature (de Gennes and Prost, 1993).

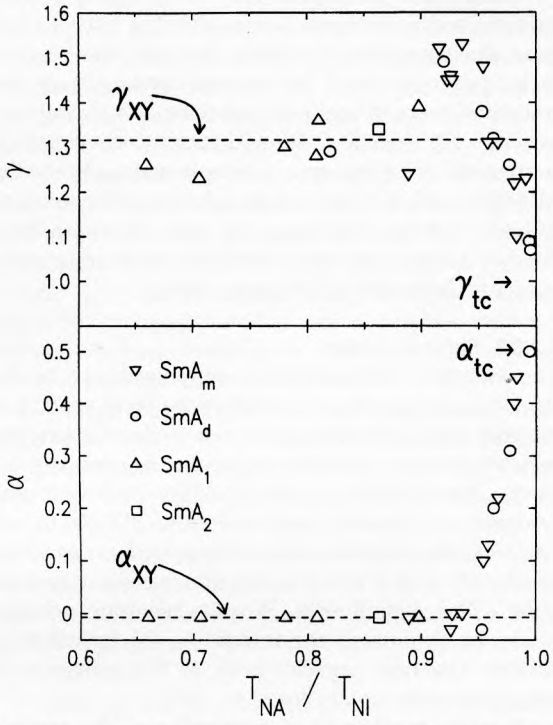


FIGURE 4.14. Specific heat exponent ($\alpha$) and susceptibility exponent ($\gamma$) as a function of the ratio of the N–A transition temperature ($T_{NA}$) to the N–I transition temperature ($T_{NI}$). (From Garland and Nounesis, 1994.)

If one looks at the measurements of continuous smectic A–nematic transitions, the critical exponents are clearly dependent on the McMillan ratio. For all ratios below about 0.93, they are close to those of the 3D XY universality class ($\alpha = -0.007$, $\gamma = 1.316$, $\nu_{\|} = \nu_{\perp} = 0.669$). Above a ratio of roughly 0.93, they are no longer fairly constant, but tend to approach their tricritical values ($\alpha = 0.5, \gamma = 1.0, \nu_{\|} = \nu_{\perp} = 0.5$) as the McMillan ratio approaches unity. This trend for $\alpha$ and $\gamma$ is shown in FIGURE 4.14. In addition, the correlation is no longer isotropic at these high McMillan ratios, with $\nu_{\|}$ falling above and $\nu_{\perp}$ falling below their tricritical values. It should be pointed out that the value of the McMillan ratio at the tricritical point is not universal and that the crossover from 3D XY values to tricritical values is not the same for different homologous series, but the trend in the critical exponents is very similar for all compounds studied. A clear demonstration

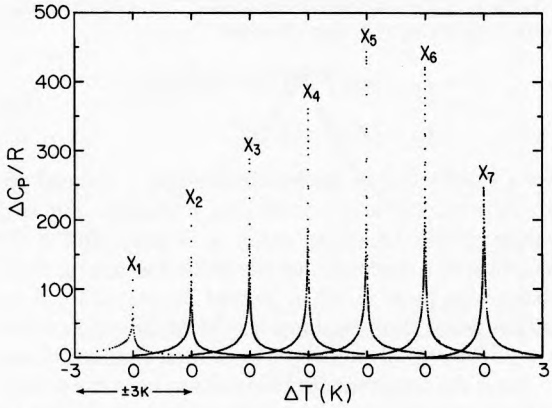


FIGURE 4.15. Excess specific heat near the nematic–smectic A transition for seven different binary mixtures. The mole fraction for one of the compounds increases from 0 ($X_1$) to 0.5 ($X_7$). (From Stine and Garland, 1989b.)

showing the change in $\alpha$ in approaching the tricritical point along with the increase in the size of the specific heat anomaly is given in FIGURE 4.15. For this binary mixture, the tricritical concentration is close to the one labeled $X_5$ in the figure.

#### 4.2.3.2 Theory

The mean-field description for the smectic A–nematic transition begins with an expansion for the free energy in terms of the amplitude of the smectic order parameter $|\psi|$

$$F = F_0 + \tfrac{1}{2}a|\psi|^2 + \tfrac{1}{4}b_0|\psi|^4 + \cdots \qquad (4.22)$$

where $a = a_0(T - T_{NA})$ and $b_0 > 0$. Only even powers are allowed since changing the sign of $|\psi|$ is the same as changing the reference point for the sinusoidal density variation and therefore cannot affect the free energy. This free energy predicts a continuous transition at $T_{NA}$.

Coupling between the amount of nematic order (given by the order parameter $S$) and the smectic order parameter $|\psi|$ complicates the theory. This means that the value of $S$ which minimizes the nematic free energy, $S_0$, may not be the value of $S$ which minimizes the total free energy if a term coupling $S$ and $|\psi|$ is present. Letting $\Delta S = S - S_0$, the free energy becomes

$$F = F_0 + \tfrac{1}{2}a|\psi|^2 + \tfrac{1}{4}b_0|\psi|^4 + \frac{(\delta S)^2}{2\chi} - c|\psi^2|(\delta S) \qquad (4.23)$$

where $\chi$ is the susceptibility and $c > 0$. Minimizing $F$ with respect to $\Delta S$, one obtains

$$F = F_0 + \tfrac{1}{2}a|\psi|^2 + \tfrac{1}{4}(b_0 - 2c^2\chi)|\psi|^4 = F_0 + \tfrac{1}{2}a|\psi|^2 + \tfrac{1}{4}b|\psi|^4. \quad (4.24)$$

For a small value of the McMillan ratio, $\chi$ is small and $b > 0$, resulting in a continuous transition. For high values of the McMillan ratio, $\chi$ is large and $b < 0$, resulting in a discontinous transition (assuming that a sixth-order term in $|\psi|$ is present for stability). A tricritical point thus exists at the McMillan ratio where $b = 0$. The critical exponents have their classical values.

Near the transition, fluctuations in both the smectic order parameter and nematic director are important. If one introduces gradient terms of the smectic order parameter into the free-energy expression but with isotropic coefficients, the situation is analogous to superfluid helium and thus 3D XY behavior is expected (Prost, 1984). If fluctuations of the director are also included, the situation resembles the normal superconducting transition. Some of the analogies to superconductivity are quite interesting. For example, just as a superconductor expells magnetic fields (the Meissner effect), smectic A liquid crystals expell twist and bend distortions. Accordingly, the twist and bend elastic constants in the nematic phase diverge as the transition to the smectic A phase is approached.

A variety of conclusions have been reached through theoretical work on this problem. The transition seems always to be first-order in four dimensions due to the coupling between the smectic order parameter and the director fluctuations (Halperin et al., 1974). In three dimensions, the behavior on the low and high sides of the transition can be reversed from 3D XY behavior, i.e., an inverted 3D XY model (Dasgupta and Halperin, 1981; and Lubensky, 1983). A dislocation-loop melting theory, in which a divergence in the density of dislocation loops destroys the smectic order, yields anisotropic critical behavior in the correlation lengths (Nelson and Toner, 1981; and Toner, 1982). Noninverted behavior is seen in Monte Carlo simulations (Dasgupta, 1987). Finally, self-consistent one-loop theory employing intrinsically anisoptropic coupling between the director fluctuations and the smectic order parameter predicts a gradual crossover from isotropic behavior to strongly anisotropic behavior (Patton and Andereck, 1992; and Andereck and Patton, 1994).

Clearly the nematic–smectic A transition is very complicated, with many factors affecting the behavior near the transition. Coupling between the smectic order parameter and the nematic order drives the transition toward tricritical behavior, while coupling between the smectic order and nematic director fluctuations drives it into an anisotropic regime. While the McMillan ratio is a convenient indicator of the strength of both of these couplings, it is quite imprecise. Still, general trends with the McMillan ratio are plainly evident (Garland and Nounesis, 1994).

#### 4.2.3.3 Polar Smectics

The smectic A phase of polar compounds can be $A_1$, A2, or $A_d$, depending on whether the layer spacing is roughly one molecular length, two molecular lengths, or between one and two molecular lengths, respectively. The smectic $A_d$–N transition falls into the category of crossover behavior from 3D XY to tricritical as the McMillan ratio is increased as described previously, and in fact this transition has been used for quite a few experiments. When a reentrant nematic phase, $N_r$, is present, the smectic $A_d$–$N_r$ transition is similar. The heat capacity peak at this transition is often extremely small (Wu et al., 1992).

A large number of experiments on the smectic $A_1$–N transition show critical exponents consistent with the 3D XY universality class (Garland, 1990). Typical specific heat data are contained in FIGURE 4.16. One of the reasons for this may be the large

FIGURE 4.16. Specific heat associated with the smectic $A_1$–nematic transition. (From Garland et al., 1989.)

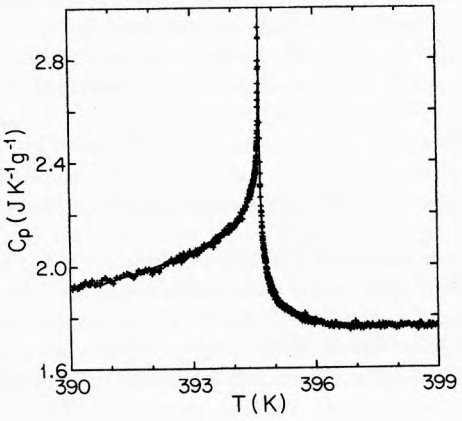

nematic range that occurs in many of these systems. More recent heat capacity measurements have also shown a tendency for this system to crossover to tricritical-like behavior (Wu et al., 1992). The reason for this may be the same as for the smectic A–N transition in nonpolar compounds (or the smectic $A_d$–N transition for polar compounds), namely a trend to a larger nematic susceptibility that drives the transition toward first order through the coupling of the nematic and smectic order parameters. For the smectic $A_1$–N transition, however, the larger nematic susceptibility may be due to a nearby nematic (dimers)–nematic (monomers) transition rather than a nearby nematic–isotropic transition.

Although most smectic $A_2$–N transitions are first-order with high values of the McMillan ratio, at least one continuous transition has been observed (Wen et al., 1991). In this case 3D XY critical exponents were obtained from heat capacity measurements. As with the other smectic–nematic transitions, it is expected that crossover from 3D XY to tricritical behavior occurs for the smectic $A_2$–N transition also. So far, experimental results showing this have not been reported.

It must be pointed out that the reentrant phenomenon in the case of polar molecules creates some very special circumstances that have only been hinted at in the previous discussion. An isolated nematic region replacing a critical point at the end of a smectic $A_d$–smectic $A_1$ coexistence line in binary mixtures has been theoretically described by a dislocation loop melting model (Prost and Toner, 1987) and experimentally observed (Hardouin et al., 1986; and Wu et al., 1992). A frustrated spin-gas model also predicts such a "nematic lake," but completely surrounded by the smectic $A_d$ phase (Marko et al., 1989). The dislocation loop melting theory also predicts that a transition between a nematic phase with strong $A_1$ fluctuations, $N_1$, to a nematic phase with strong $A_d$ fluctuations, $N_d$, occurs in this region, but such a transition has not been observed.

In the case of mixtures, especially ones involving dissimilar molecules, Fischer renormalization is sometimes important (Fischer, 1968; and Anisimov, 1988). This is a renormalization of the critical exponents in systems with positive $\alpha$ due to large changes in the smectic A–nematic transition temperature as the concentration is varied. The critical exponents are divided by $1 - \alpha$, except for $\alpha$ itself, which is divided by $\alpha - 1$.

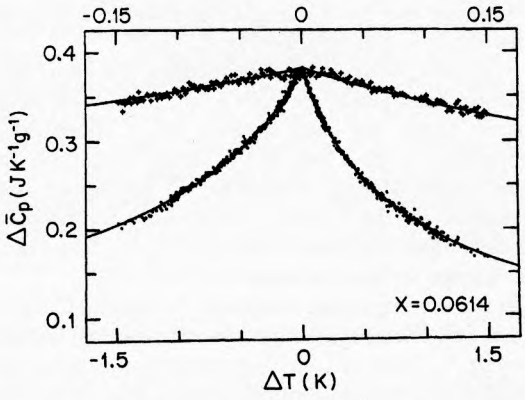


FIGURE 4.17. Excess specific heat at the smectic $A_d$–nematic transition for a tricritical mixture. The solid line is a fit with a fully Fischer-renormalized exponent. (From Huster et al., *Phys. Rev. A* 36, 2364 (1987)).

Good examples of this occur in mixtures of polar and nonpolar molecules (Huster et al., 1987; Hill et al., 1989; and Stine and Garland, 1989). FIGURE 4.17 shows heat capacity data for the tricritical mixture of two dissimilar molecules. The data fit a curve with a renormalized value for $\alpha$ of $-1$.

### 4.2.4 Smectic A–Smectic C Transitions

The order parameter that must be specified in the smectic A–smectic C transition is the magnitude and azimuthal direction of the tilt of the director relative to the layer normal. Thus a two-component (complex) order parameter and free energy are involved, both of which are formally identical to the condensation of superfluid helium (de Gennes, 1972). This leads to the expectation that the transition is continuous and of the 3D XY universality class. The heat capacity critical exponent should be about $-0.007$ and below the transition the tilt angle should vary with temperature with a power of about 0.35.

The regime of critical fluctuations, however, may lie outside of experimental observation. The Ginzburg criterion indicates that for this transition a reduced temperature as low as $10^{-5}$ may be necessary to observe critical phenomena. The experimental data show mean-field Landau behavior with a large sixth-order term (Huang and Viner, 1982; and Birgeneau et al., 1983). The heat capacity exponent $\alpha$ is too small

to measure and the tilt angle dependence below the transition is in the neighborhood of 0.35.

In smectic A–smectic C* transitions, the lower temperature phase possesses both a helicoidal twist of the director about the layer normal and a spontaneous polarization in the plane of the layers. Both first- and second-order smectic A–smectic C* transitions have been observed; the continuous transitions and tricritical point are again explained well by a Landau free energy with a large sixth-order term (Garland, 1992).

In polar compounds a smectic A–smectic C transition is possible, but in both cases involving bilayers (smectic $A_2$–smectic $C_2$). Heat capacity studies on this transition for two compounds show a step in the heat capacity at the transition with a constant value below the transition. A mean-field model for the data in the smectic $A_2$ phase requires an extremely small sixth-order term (Jeong et al., 1988; and Wen et al., 1991).

## 4.2.5 Nematic–Smectic A–Smectic C Point

By varying the concentration in a binary mixture or by varying the pressure in certain single-component systems, it is possible to obtain a point where the smectic A–N, smectic A–smectic C, and smectic C–N phase boundaries meet (NAC point). This region of the phase diagram has been studied extensively, with very interesting results.

Perhaps the most important finding is that there is universal behavior near the NAC point. FIGURE 4.18 shows that the phase diagrams for four different binary systems fall right on top of each other (Brisbin et al., 1983; Shashidhar et al., 1984). FIGURE 4.19 shows that a single-component system under pressure has the same topology in the neighborhood of the NAC point (Shashidhar et al., 1984). The boundaries between the phases in a temperature ($T$)–concentration ($X$) phase diagram obey simple power laws of the form

$$T - T_{NAC} = A|X - X_{NAC}|^{\phi} + B(X - X_{NAC}), \qquad (4.25)$$

where $A$ and $B$ are constants and $\phi$ is equal to about 0.6 for the smectic A–N and smectic C–N transitions, and about 1.5 for the smectic A–smectic C transition. An NAC point also exists for some reentrant nematic phases. In many cases the critical regions near this NAC point seem too small to be realized, but in the proper system singularities in the phase boundaries and the same universal behavior have been observed (Somasekhara et al., 1986).

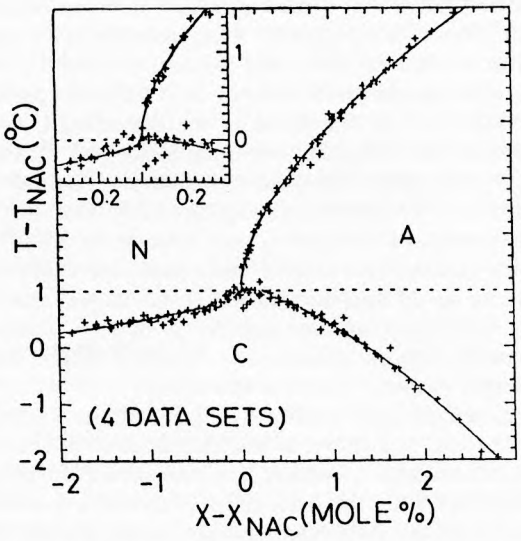


FIGURE 4.18. Temperature–concentration phase diagram in the vicinity of the NAC point for four binary mixtures. (From Shashidhar et al., *Phys. Rev. Lett.* 53, 2141 (1984)).

### 4.2.5.1 Theory

Any theoretical description of the NAC point must utilize an order parameter which can describe a mass density wave not just normal to the layers, but in rings

FIGURE 4.19. Temperature–pressure phase diagram in the vicinity of the NAC point for a single compound. (From Shashidhar et al., 1984.)

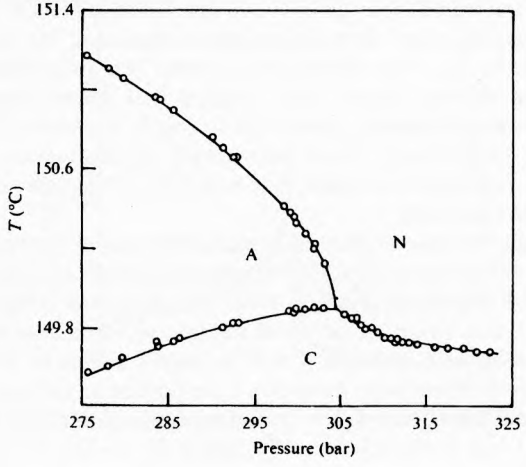

around the layer normal. A single order parameter involving an integration in wavevector space can be used in a free energy involving this order parameter and gradients of this order parameter (Chen and Lubensky, 1976). Depending on the sign of one of the coefficients, the fluctuations in the nematic phase can be either smectic A-like or smectic C-like. The point where both this coefficient and the coefficient in front of the term quadratic in the order parameter are zero is the NAC point and implies that the NAC point is a Lifshitz point (Hornreich et al., 1975). The amplitude of the mass density wave increases in moving away from the Lifshitz point and the x-ray scattering profile should change from being Lorentzian away from the NAC point to quartic at the NAC point. Other theoretical approaches utilize two order parameters, one for the mass density wave and the other for the tilt angle.

A dislocation loop model can be developed by using the renormalization group technique (Grinstein and Toner, 1984). The interesting addition in this treatment is the prediction of a biaxial nematic phase between the nematic and smectic C phases. This means that the NAC point is really a tetracritical point. The theory of Chen and Lubensky can also be modified to predict such a biaxial nematic phase if fluctuations are included (Grinstein et al., 1986).

#### 4.2.5.2 Experiment

The NAC point has been investigated most thoroughly using calorimetry but there have been some high-resolution x-ray scattering and light scattering experiments also. The first detailed study was done on a binary mixture of two thioesters, revealing second-order smectic A–N and smectic C–smectic A transitions and a first-order smectic C–N transition, although the latent heat for this last transition decreased to zero at or near the NAC point (De Hoff et al., 1982). Experiments on other systems confirm these first results and the nature of the heat capacity anomalies indicate that a classical tricritical point may exist at or near the NAC point (Anisimov et al., 1985; Garland and Huster, 1987; and Thoen and Parret, 1989). Alternatively, the x-ray scattering (Safinya et al., 1981, 1983; and Martinez-Miranda et al., 1986) and light scattering experiments (Witanachi et al., 1983; Solomon and Litster, 1987; and Huang and Ho, 1987, 1990) are in full agreement with the NAC point being a Lifshitz point.

Although the biaxial nematic phase between the nematic and smectic C phases has not been observed, a broad peak in the heat capacity in the nematic phase has been observed in two systems. The first was a binary mixture of two nonchiral compounds (Anisimov et al., 1985) and the second was a binary mixture of two chiral substances with chiral nematic and chiral smectic C phases (Wen et al., 1990). These broad peaks may be the manifestation of biaxial or chiral fluctuations.

### 4.2.6 Smectic A–Hexatic Smectic B Transition

The order that sets in at the smectic A–hexatic smectic B phase transition is bond orientational order with sixfold symmetry in the plane of the layers. The appropriate order parameter is much like the smectic A order parameter, namely a bond angle variation of the form

$$\psi_6 = I_6 \, e^{6i\phi} \tag{4.26}$$

where $\phi$ is the azimuth angle and $I_6$ is the complex order parameter. This complex order parameter should again put the transition into the 3D XY universality class. However, instead of a critical exponent $\alpha$ near $-0.007$, heat capacity and optical studies yield values for $\alpha$ of about 0.6 (Pitchford et al., 1985; and Nounesis et al., 1986). The heat capacity data can be seen in FIGURE 4.20. While these results are clearly inconsistent with the 3D XY model, they are close to the tricritical value of 0.5, raising the question of whether the transition occurs in the neighborhood of a tricritical point. In order to predict such a tricritical

FIGURE 4.20. Specific heat in the vicinity of a hexatic B–smectic A transition. (From Nounesis et al., 1986.)

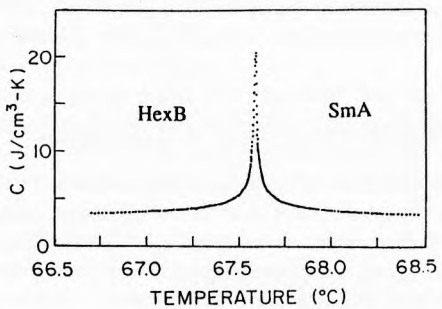

point, theoretical work includes a coupling of $I_6$ to some other type of local order, but more recent heat capacity results show that this high value of $\alpha$ is maintained over wide composition ranges and in many compounds, making the explanation of a tricritical point less likely (Huang et al., 1989; and Nounesis et al., 1989).

The transition to hexatic order has also been studied in tilted phases. In this case the transition is from the smectic C phase to either the smectic F or smectic I phases. The molecular tilt acts as a temperature-independent field, which promotes some bond orientational order in the smectic C phase. In at least one compound the heat capacity peak at the smectic C–smectic I transition is clearly rounded (Garland et al., 1989), while in other compounds the smectic C–smectic F transition is strongly first-order (Stine and Garland, 1990).

Some recent work on free-standing liquid crystal films has been very revealing. For very thin smectic A films of three or four layers, a single heat capacity peak appears at the smectic A–hexatic B transition. For thicker films (five to ten layers) two heat capacity peaks appear, one at a higher temperature representing the establishment of bond orientational order in the outer two layers and another at lower temperature when the rest of the film undergoes the phase transition (Geer et al., 1989). These thinnest films with only one heat capacity peak have the chance of representing a truly two-dimensional system. The record for the number of individual layer transitions observed is four. Using a different compound in the same homologous series, heat capacity studies have revealed the smectic A–hexatic B transition at 74 °C for the outermost layers, 67 °C for the second outermost layers, 66.3 °C for the third outermost layers, and the fourth outermost layers transforming just above the bulk transition. These layer transitions are evident in the data shown in FIGURE 4.21 (Geer et al., 1993). All these layer transitions are continuous (Stoebe et al., 1992).

## 4.2.7 Smectic A–Smectic A Transitions

The large number of smectic phases exhibited by polar molecules creates many interesting phase diagrams. Many involve transitions between different smectic A phases as well as interesting critical points, reentrant phases, and isolated nematic regions.

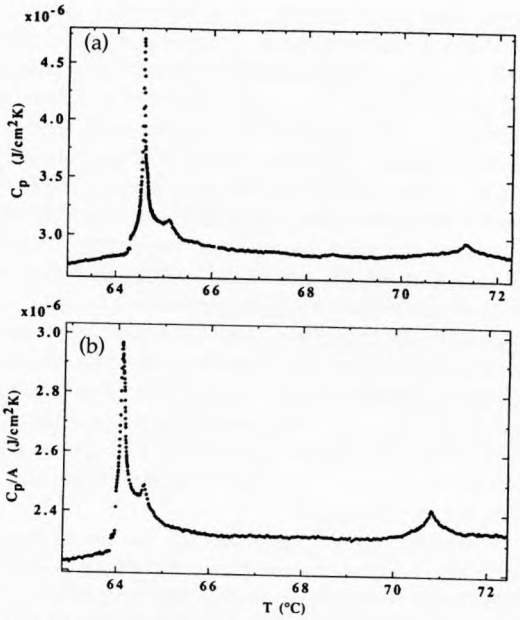


FIGURE 4.21. Specific heat near the hexatic B–smectic A transition in thin films. (a) Ten layers and (b) eight layers. (From Geer et al., *Phys. Rev. E* 48, 408 (1993)).

### 4.2.7.1 Smectic $A_1$–Smectic $A_2$ Transition

The transition from the smectic $A_1$ phase to the smectic $A_2$ phase involves the doubling of the spatial period due to dipolar ordering, so it can be first- or second-order. Theoretical work places this transition in the 3D Ising universality class with critical exponents $\gamma = 1.24$, $\nu = 0.63$, and $\alpha = 0.11$ (Prost and Barois, 1983; and Wang and Lubensky, 1984). Heat capacity and high-resolution x-ray studies in binary mixtures of a nonpolar and a polar compound have observed a tricritical point where the transition changes from first- to second-order, but the measured exponents have significantly different values, namely $\gamma = 1.46 \pm 0.05$, $\nu = 0.74 \pm 0.03$, and $\alpha \simeq -0.16$ (Chan et al., 1986; and Das et al., 1990). These different results can be nicely explained by Fischer renormalization, since the slope of the temperature–concentration phase boundary is large (Fischer, 1968; Anisimov, 1988). When the renormalized values of the critical exponents are calculated, one obtains $\gamma = 1.39$, $\nu = 0.71$, and $\alpha = -0.124$, which are all close to the measured values. FIGURE 4.22 shows the heat capacity data.

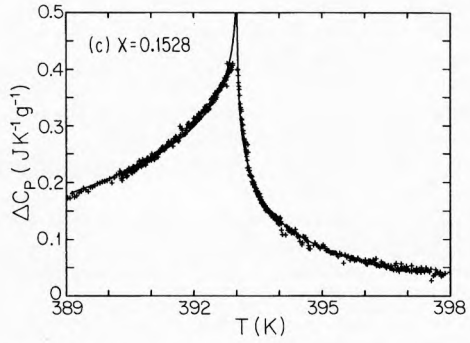


FIGURE 4.22. Excess specific heat associated with the smectic $A_2$–smectic $A_1$ transition. (From Das et al., 1990.)

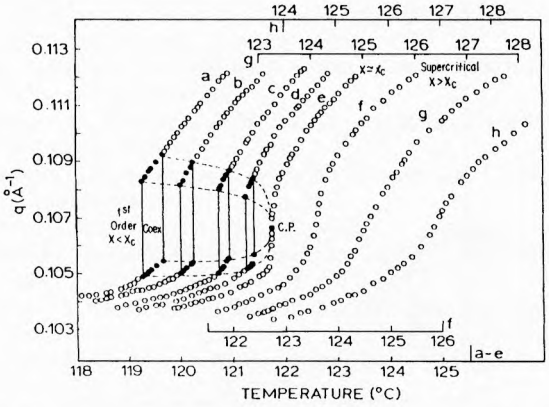


FIGURE 4.23. Smectic wavevector in the vicinity of the smectic $A_d$–smectic $A_2$ transition for eight binary mixtures. (From Shashidhar et al., 1987.)

#### 4.2.7.2 Smectic $A_d$–Smectic $A_2$ Transition

The smectic $A_d$ and smectic $A_2$ phases both involve dipolar ordering of pairs of molecules in layers, so they possess the same macroscopic symmetry. The phase boundary between them must represent a first-order transition and the boundary can end at a critical point. This has been confirmed by x-ray measurements that measured the layer periodicities in the neighborhood of the transition. In a binary mixture of two polar compounds, changing the temperature for certain mixtures caused the transition to take place. As this was repeated for differing concentrations, what was a discontinuous jump in the layer spacing at the transition (with a two-phase region) became less and less of a jump, finally reaching a critical concentration for which one phase continuously evolved into the other phase (Shashidhar et al., 1987). This behavior, which is shown in FIGURE 4.23, is strikingly similar to what happens to the density at the gas–liquid critical point. Theoretical arguments involving fluctuations and order parameter coupling to the elastic degrees of freedom, however, suggest that this critical point may belong to a new universality class with upper critical dimension six and anisotropic scaling (Park et al., 1988). Experiments seem to confirm this (Prost et al., 1990; and Wen et al., 1992).

#### 4.2.7.3 Smectic $A_d$–Smectic $A_1$ Transition

In a similar fashion, it is predicted theoretically that the smectic $A_d$–smectic $A_1$ transition line can end at a critical point (Park et al., 1988). A disclination loop model, however, predicts a number of other interesting possibilities (Prost and Toner, 1987). One of them involves a "nematic lake" at the end of the smectic $A_d$–smectic $A_1$ transition line, as has been mentioned previously. This "nematic lake" is separated from the smectic phases around it by a second-order transition boundary, but the two ends of this boundary connect to the first-order smectic $A_d$–smectic $A_1$ phase transition line at two different points. This creates a first-order smectic $A_d$–N phase transition and finally a first-order N–N transition. This N–N transition line ends in the nematic lake at a critical point. Inside the nematic lake and on opposite sides of the N–N transition line, there are two nematic phases. One is characterized by strong $A_d$-type smectic fluctuations and the other by strong $A_1$-type smectic fluctuations. As is clear from FIGURE 4.24, such a "nematic lake" has been observed, but high-resolution experiments capable of detecting some of these predicted transitions have not been performed (Hardouin et al., 1986; and Wu et al., 1992).

#### 4.2.7.4 Other Transitions

Transitions are possible between both the smectic $A_1$ and smectic $A_2$ phases and the modulated antiferroelectric phases (antiphase $\tilde{A}$ or crenelated phase $A_{cren}$). The smectic $A_1$–smectic $\tilde{A}$ transition is expected to be first-order due to Brazovskii fluctuations (Prost and Barois, 1983). While two-phase coexistence has been observed for this transition, there are strong pretransitional effects, especially on the smectic $A_1$ side of the transition. The transition to the smectic $A_{cren}$ phase is

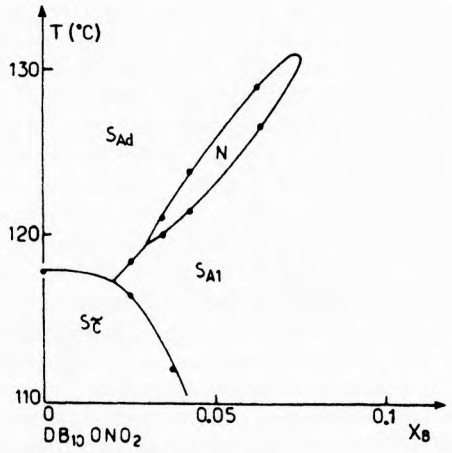


FIGURE 4.24. Partial temperature–concentration phase diagram for a binary mixture. (From Hardouin et al., 1986.)

very different, with a heat capacity peak which is truncated. The interpretation is that the smectic $A_{cren}$ phase is more like a periodic repeating of smectic $\tilde{A}$ and smectic $A_2$ slabs (Garland, 1990).

It should be noted that all smectic A phases possess the same macroscopic symmetry. One way to realize this comes from the fact that the smectic $A_1$ phase can convert to the smectic $A_d$ phase without a phase transition and that the smectic $A_d$ phase can convert without a phase transition to the smectic $A_2$ phase. Therefore, it is possible for the smectic $A_1$ phase to convert to the smectic $A_2$ phase without a phase transition. This does not rule out, however, the possibility of a first- or second-order transition from the smectic $A_1$ to the smectic $A_2$ phase (de Gennes and Prost, 1993).

## REFERENCES


Als-Nielsen, J., Litster, J. D., Birgeneau, R. J., Kaplan, M., Safinya, C. R., Lindegaard, A., and Mathiesen, S. 1980. *Phys. Rev. B* **22**: 312.

Andereck, B. S., and Patton, B. R. 1994. *Phys. Rev. E* **49**: 1393.

Anisimov, M. A., Voronov, V. P., Kulkov, A. O., and Kholmurodov, F. 1985. *J. Physique* **46**: 2137.

Anisimov, M. A., Labko, V. I., Nikolaenko, G. L., and Yudin, I. K. 1987. *Sov. Phys.–JETP* **45**: 111.

Anisimov, M. A. 1988. *Mol. Cryst. Liq. Cryst.* **162A**: 1.

Anisimov, M. A., Cladis, P. E., Gorodetskii, E. E., Huse, D. A., Podneks, V. E., Taratuta, V. G., van Saarloos, W., and Voronov, V. P. 1990. *Phys. Rev. A* **41**: 6749.

Birgeneau, R. J., Garland, C. W., Kortan, A. R., Lister, J. D., Meichle, M., Ocko, B. M., Rosenblatt, C., Yu, L. J., and Goodby, J. W. 1983. *Phys. Rev. A* **27**: 1251.

Birgeneau, R. J., Garland, C. W., Kortan, A. R., Litster, J. D., Meichle, M., Ocko, B. M., Rosenblatt, C., Yu, L. J., and Goodby, J. W. 1984. *Phys. Rev. A* **29**: 1371.

Bowling, M. B., Collings, P. J., Booth, C. J., and Goodby, J. W. 1993. *Phys. Rev. E* **48**: 4113.

Brazovskii, S. A., and Dmitriev, S. G. 1975. *Zh. Eksp. Teor. Fiz.* **69**: 979 (1976. *Sov. Phys.–JETP* **42**: 497).

Brazovskii, S. A., and Filev, V. M. 1978. *Zh. Eksp. Teor Fiz.* **75**: 1140 (1978. *Sov. Phys.–JETP* **48**: 573).

Brisbin, D., Johnson, D. L., Fellner, H., and Neubert, M. E. 1983. *Phys. Rev. Lett.* **50**: 178.

Caillé, A. 1972. *C. R. Acad. Sci. Paris B* **274**: 891.

Chan, K. K., Pershan, P. S., Sorensen, L. B., and Hardouin, F. 1986. *Phys. Rev. A* **34**: 1420.

Chandari, A. D. L., Ouchi, Y., Takezoe, H., Fukuda, A., Terashima, K., Furukawa, K., and Kishi, A. 1989. *Japan. J. Appl. Phys. Lett.* **28**: 1261.

Chandrasekhar, S., Sadashiva, B. K., Ramesha, S., and Srikanta, B. S. 1986. *Pramana* **27**: L713.

Chandrasekhar, S., and Ranganath, G. S. 1990. *Rep. Prog. Phys.* **53**: 57.

Chandrasekhar, S. 1992. *Liquid Crystals.* 2d ed. Cambridge: Cambridge University Press.

Chen, J. H., and Lubensky, T. C. 1976. *Phys. Rev. A* **14**: 1202.

Chen, W., Martinez-Miranda, L. J., Hsiung, H., and Shen, Y. R. 1989. *Phys. Rev. Lett.* **62**: 1860.

Cladis, P. E. 1975. *Phys. Rev. Lett.* **35**: 48.

Cladis, P. E., Bogardus, R. K., Daniels, W. B., and Taylor, G. N. 1977. *Phys. Rev. Lett.* **39**: 720.

Cladis, P. E. 1980. *Liquid Crystals: Proceedings of an International Conference Held at the Raman Research Institute [Bangalore 1979]*, ed. S. Chandrasekhar, p. 105. London: Heyden.

Cladis, P. E., van Saarloos, W., Huse, D. A., Patel, J. S., Goodby, J. W., and Finn, P. L. 1989. *Phys. Rev. Lett.* **62**: 1764.

Collings, P. J. 1992. *Mod. Phys. Lett. B* **6**: 425.

Crooker, P. P. 1989. *Liq. Cryst.* **5**: 751.

Das, P., Nounesis, G., Garland, C. W., Sigaud, G., and Tinh, N. H. 1990. *Liq. Cryst.* **7**: 883.

Dasgupta, C. 1987. *J. Phys.* **48**.

Dasgupta, C., and Halperin, B. I. 1981. *Phys. Rev. Lett.* **47**: 1556.

de Gennes, P. G. 1972a. *C. R. Acad. Sci. Paris B* **274**: 758.

de Gennes, P. G. 1972b. *Solid State Commun.* **10**: 753.

de Gennes, P. G., and Prost, J. 1993. *The Physics of Liquid Crystals.* 2d ed. Oxford: Oxford University Press.

De Hoff, R., Biggers, R., Brisbin, D., and Johnson, D. L. 1982. *Phys. Rev. A* **25**: 472.

Destrade, C., Tinh, N. H., Malthete, J., and Jacques, J. 1980. *Phys. Lett.* **79A**: 189.

Emsley, J. W., ed. 1985. *NMR of Liquid Crystals.* Darmstadt: Reidel.

Fischer, M. E. 1968. *Phys. Rev.* **176**: 257.

Fontes, E., Heiney, P. A., and de Jeu, W. H. 1988. *Phys. Rev. Lett.* **61**: 1202.

Frank, F. C., and Chandrasekhar, S. 1980. *J. Physique* **41**: 1285.

Garland, C. W. 1992. *Phase Transitions in Liquid Crystals,* eds. S. Martellucci and A. N. Chester, p. 175. New York, Plenum.

Garland, C. W., and Huster, M. E. 1987. *Phys. Rev. A* **35**: 2365.

Garland, C. W., Litster, J. D., and Stine, K. J. 1989. *Mol. Cryst. Liq. Cryst.* **170**: 71.

Garland, C. W. 1990. *Geometry and Thermodynamics,* ed. J.-C. Tolédano, p. 221. New York: Plenum.

Garland, C. W., and Nounesis, G. 1994. *Phys. Rev. E* **49**: 2964.

Geer, R., Huang, C. C., Pindak, R., and Goodby, J. W. 1989. *Phys. Rev. Lett.* **63**: 540.

Geer, R., Stoebe, T., Huang, C. C., and Goodby, J. W. 1992. *Phys. Rev. A* **46**: 6162.

Geer, R., Stoebe, T., and Huang, C. C. 1993. *Phys. Rev. E* **48**: 408.

Gohin, A., Destrade, C., Gasparoux, H., and Prost, J. 1983. *J. Physique* **44**: 427.

Goodby, J. W., Waugh, M. A., Stein, S. M., Chin, E., Pindak, R., and Patel, J. S. 1989. *J. Am. Chem. Soc.* **111**: 8119.

Gorecka, E., Chandani, A. D. L., Ouchi, Y., Takezoe, H., and Fukuda, A. 1990. *Japan. J. Appl. Phys.* **29**: 131.

Grebel, H., Hornreich, R. M., and Shtrikman, S. 1983. *Phys. Rev. A* **28**: 1114.

Grebel, H., Hornreich, R. M., and Shtrikman, S. 1984. *Phys. Rev. A* **30**: 3264.

Grinstein, G., and Toner, J. 1984. *Phys. Rev. Lett.* **51**: 2386.

Grinstein, G., Lubensky, T. C., and Toner, J. 1986. *Phys. Rev. B* **33**: 3306.

Halperin, B. I., Lubensky, T. C., and Ma, S.-K. 1974. *Phys. Rev. Lett.* **32**: 292.

Halperin, B. I., and Nelson, D. R. 1978. *Phys. Rev. Lett.* **41**: 121.

Hardouin, F., Achard, M. F., Nguyen, H. T., and Sigaud, G. 1986. *Mol. Cryst. Liq. Cryst. Lett.* **3**: 7.

Hill, J. P., Keimer, B., Evans-Lutterodt, K. W., Birgeneau, R. J., and Garland, C. W. 1989. *Phys. Rev. A* **40**: 4625.

Hornreich, R. M., Luban, M., and Shtrikman, S. 1975. *Phys. Rev. Lett.* **35**: 1678.

Hornreich, R. M., and Shtrikman, S. 1989. *Mol. Cryst. Liq. Cryst.* **165**: 183.

Huang, C. C., and Viner, J. M. 1982. *Phys. Rev. A* **25**: 3385.

Huang, C. C., Nounesis, G., Geer, R., Goodby, J. W., and Guillon, D. 1989. *Phys. Rev. A* **39**: 3741.

Huang, J., and Ho, J. T. 1987. *Phys. Rev. Lett.* **58**: 2239.

Huang, J., and Ho, J. T. 1990. *Phys. Rev. A* **42**: 2449.

Huster, M. E., Stine, K. J., and Garland, C. W. 1987. *Phys. Rev. A* **36**: 2364.

Ihn, K. J., Zasadzinski, J. A. N., Pindak, R., Slaney, A. J., and Goodby, J. W. 1992. *Science* **258**: 275.

Inui, S., Kawano, S., Saito, M., Iwane, H., Takanishi, Y., Hiraoka, K., Ouchi, Y., Takezoe, H., and Fukuda, A. 1990. *Japan. J. Appl. Phys. Lett.* **29**: 987.

Jen, S., Clark, N. A., Pershan, P. S., and Priestley, E. B. 1977. *J. Chem. Phys.* **66**: 4635.

Jeong, Y. H., Stine, K. J., Garland, C. W., and Tinh, N. H. 1988. *Phys. Rev. A* **37**: 3465.

Kasting, G. B., Garland, C. W., and Lushington, K. J. 1980. *J. Physique* **41**: 879.

Keyes, P. H. 1991. *Mater. Res. Bull.* **16**: 32.

Kohli, M., Otnes, K., Pynn, R., and Riste, T. 1976. *Z. Phys. B* **24**: 147.

Kumar, S., Chen, L., and Surendranath, V. 1991. *Phys. Rev. Lett.* **67**: 322.

Kutnjak, Z., Garland, C. W., Passmore, J. L., and Collings, P. J. 1995. *Phys. Rev. Lett.* **74**: 4859.

Landau, L. D. 1965. *Collected Papers of L. D. Landau.* Ed. D. ter Haar. New York: Gordon and Breach.

Lavrentovich, O. D., and Nastishin, Y. A. 1990. *Europhys. Lett.* **12**: 135.

Lavrentovich, O. D. 1991. *Phys. Scr. T* **39**: 394.

Leadbetter, A. J. 1987. *Thermotropic Liquid Crystals,* ed. G. W. Gray, p. 1. New York: Wiley.

Levelut, A. M., Tarento, R. J., Hardouin, F., Achard, M. F., and Sigaud, G. 1981. *Phys. Rev. A* **24**: 2180.

Levelut, A. M. 1984. *J. Physique Lett.* **45**: 603.

Litster, J. D., and Stinson, T. 1972. *Phys. Rev. Lett.* **28**: 688.

Lubensky, T. C. 1983. *J. Chem. Phys.* **80**: 31.

Lubensky, T. C., Ramaswamy, S., and Toner, J. 1988. *Phys. Rev. A* **38**: 4284.

Luckhurst, G. R., and Yeates, R. N. 1976. *J. Chem. Soc. Faraday Trans. II* **72**: 996.

Marko, J. F., Indekeu, J. O., and Berker, A. N. 1989. *Phys. Rev. A* **39**: 4201.

Martinez-Miranda, L. J., Kortan, A. R., and Birgeneau, R. J. 1986. *Phys. Rev. Lett.* **56**: 2264.

McMillan, W. L. 1973. *Phys. Rev. A* **7**: 1419.

Miyano, K. 1978. *J. Chem. Phys.* **69**: 4807.

Moncton, D. E., and Pindak, R. 1979. *Phys. Rev. Lett.* **43**: 701.

Navailles, L., Barois, P., and Nguyen, H. T. 1993. *Phys. Rev. Lett.* **71**: 545.

Nelson, D. R., and Halperin, B. I. 1979. *Phys. Rev. B* **19**: 2457.

Nelson, D. R., and Toner, J. 1981. *Phys. Rev. B* **24**: 363.

Nounesis, G., Huang, C. C., and Goodby, J. W. 1986. *Phys. Rev. Lett.* **56**: 1712.

Nounesis, G., Geer, R., Lin, H. Y., Huang, C. C., and Goodby, J. W. 1989. *Phys. Rev. A* **40**: 5468.

Ocko, B. M., Birgeneau, R. J., Litster, J. D., and Neubert, M. E. 1984. *Phys. Rev. Lett.* **52**: 208.

Pang, J., Muzny, C. D., and Clark, N. A. 1992. *Phys. Rev. Lett.* **69**: 2783.

Park, Y., Lubensky, T. C., Barois, P., and Prost, J. 1988. *Phys. Rev. A* **37**: 2197.

Patel, P., Keast, S. S., Neubert, M. E., and Kumar, S. 1992. *Phys. Rev. Lett.* **69**: 301.
Patton, B. R., and Andereck, B. S. 1992. *Phys. Rev. Lett.* **69**: 1556.
Peierls, R. E. 1934. *Helv. Phys. Acta Suppl.* **2**: 81.
Pershan, P. S. 1988. *Structure of Liquid Crystal Phases*. Singapore: World Scientific.
Pindak, R., Moncton, D. E., Davey, S. C., and Goodby, J. W. 1981. *Phys. Rev. Lett.* **46**: 1135.
Pitchford, T., Nounesis, G., Dumrongrattana, S., Viner, J. M., Huang, C. C., and Goodby, J. W. 1985. *Phys. Rev. A* **32**: 1938.
Praefcke, K., Krohne, B., Singer, D., Demus, D., Pelzl, G., and Diele, S. 1990. *Liq. Cryst.* **7**: 589.
Praefcke, K., Krohne, B., Gundogan, B., Singer, D., Demus, D., Diele, S., Pelzl, G., and Bakowsky, U. 1991. *Mol. Cryst. Liq. Cryst.* **198**: 393.
Prost, J. 1979. *J. Physique* **40**: 581.
Prost, J., and Barois, P. 1983. *J. Chim. Phys.* **80**: 65.
Prost, J. 1984. *Adv. Phys.* **33**: 1.
Prost, J., and Toner, J. 1987. *Phys. Rev. A* **36**: 5008.
Prost, J., Pommier, J., Rouillon, J. C., Marcerou, J. P., Barois, P., Benzekri, M., Babeau, A., and Nguyen, H. T. 1990. *Phys. Rev. B* **42**: 2521.
Ratna, B. R., Shashidhar, R., and Raja, V. N. 1985. *Phys. Rev. Lett.* **55**: 1476.
Renn, S. R., and Lubensky, T. C. 1988. *Phys. Rev. A* **38**: 2132.
Renn, S. R. 1992. *Phys. Rev. A* **45**: 953.
Safinya, C. R., Birgeneau, R. J., Litster, J. D., and Neubert, M. E. 1981. *Phys. Rev. Lett.* **47**: 668.
Safinya, C. R., Martinez-Miranda, L. J., Kaplan, M., Litster, J. D., and Birgeneau, R. J. 1983. *Phys. Rev. Lett.* **50**: 56.
Safinya, C. R., Roux, D., Smith, G. S., Sinha, S. K., Dimon, P., Clark, N. A., and Bellocq, A. M. 1986. *Phys. Rev. Lett.* **57**: 2718.
Seideman, T. 1990. *Rep. Prog. Phys.* **53**: 659.
Shashidhar, R., Ratna, B. R., and Prasad, S. K. 1984. *Phys. Rev. Lett.* **53**: 2141.
Shashidhar, R., Ratna, B. R., Prasad, S. K., Somasekhara, S., and Heppke, G. 1987. *Phys. Rev. Lett.* **59**: 1209.
Sirota, E. B., Pershan, P. S., Sorensen, L. B., and Collett, J. 1987. *Phys. Rev. A* **36**: 2890.
Solomon, L., and Litster, J. D. 1987. *Phys. Rev. Lett.* **56**: 2268.
Somasekhara, S., Shashidhar, R., and Ratna, B. R. 1986. *Phys. Rev. A* **34**: 2561.
Stine, K. J., and Garland, C. W. 1989a. *Phys. Rev. A* **39**: 1482.
Stine, K. J., and Garland, C. W. 1989b. *Phys. Rev. A* **39**: 4919.
Stine, K. J., and Garland, C. W. 1990. *Mol. Cryst. Liq. Cryst.* **188**: 91.
Stoebe, T., Geer, R., Huang, C. C., and Goodby, J. W. 1992. *Phys. Rev. Lett.* **69**: 2090.
Thoen, J., Marynissen, H., and Van Dael, W. 1984. *Phys. Rev. Lett.* **52**: 204.
Thoen, J., and Parret, R. 1989. *Liq. Cryst.* **5**: 479.
Thoen, J. 1992. *Phase Transitions in Liquid Crystals*, ed. S. Martellucci and A. N. Chester, p. 155. New York: Plenum.
Tinh, N. H., Hardouin, F., Destrade, C., and Levelut, A. M. 1982. *J. Physique Lett.* **43**: 33.
Toner, J. 1982. *Phys. Rev. B* **26**: 462.
Voets, G. 1992. *PhD Thesis*, University of Louvain.
Voets, G., and Van Dael, W. 1993. *Liq. Cryst.* **14**: 617.
Wang, J., and Lubensky, T. C. 1984. *Phys. Rev. A* **29**: 2210.
Wen, X., Garland, C. W., and Wand, M. D. 1990. *Phys. Rev. A* **42**: 6087.
Wen, X., Garland, C. W., and Heppke, G. 1991. *Phys. Rev. A* **44**: 5064.
Wen, X., Garland, C. W., Shashidhar, R., and Barois, P. 1992. *Phys. Rev. B* **45**: 5131.
Witanachi, W., Huang, J., and Ho, J. T. 1983. *Phys. Rev. Lett.* **50**: 594.
Wright, D. C., and Mermin, N. D. 1989. *Rev. Mod. Phys.* **61**: 385.
Wu, L., Garland, C. W., and Pfeiffer, S. 1992. *Phys. Rev. A* **46**: 973.
Yang, D. K., and Crooker, P. P. 1987. *Phys. Rev. A* **35**: 4419.
Young, A. P. 1979. *Phys. Rev. B* **19**: 1855.
Young, M. J., Wu, L., Nounesis, G., Garland, C. W., and Birgeneau, R. J. 1994. *Phys. Rev. E* **50**: 368.
Yu, L. J., and Saupe, A. 1980. *Phys. Rev. Lett.* **45**: 1000.